

МІНІСТЕРСТВО ОСВІТИ І НАУКИ УКРАЇНИ
НАЦІОНАЛЬНИЙ ТЕХНІЧНИЙ УНІВЕРСИТЕТ УКРАЇНИ
“КИЇВСЬКИЙ ПОЛІТЕХНІЧНИЙ ІНСТИТУТ ІМ. ІГОРЯ СІКОРСЬКОГО ”
Факультет електроніки
Кафедра електронної інженерії

До захисту допущено
Завідувач кафедри
В. І. Тимофєєв
“ ” 20__ р.

Дипломна робота

освітнього рівня «бакалавр»
за спеціальністю 153 мікро- та наносистемна техніка


на тему «Аналіз електроенцефалограм людини,
отриманих під час емоційних стимулів»

Виконав студент 4 курсу, групи ДМ-72


Водяник Богдан Романович
(прізвище, ім'я, по батькові)


(підпис)

Керівник доц. каф. ЕІ, доц., к.т.н. А.О. Попов
(посада, вчене звання, науковий ступінь, прізвище та ініціали)


(підпис)

Рецензент доц. каф. ЕПС, доц., к.т.н. К.С. Клен
(посада, вчене звання, науковий ступінь, прізвище та ініціали)


(підпис)

Засвідчую, що у цій дипломній роботі немає
запозичень з праць інших авторів без відповідних
посилань.

Студент 
(підпис)

Київ - 2021 року

Форма № Н-9.01

**Національний технічний університет України
“Київський політехнічний інститут імені Ігоря Сікорського”**

Факультет електроніки
Кафедра електронної інженерії
Освітній рівень «бакалавр»
за спеціальністю 153 мікро- та наносистемна техніка

ЗАТВЕРДЖУЮ

Завідувач кафедри

_____ В. І. Тимофєєв
“ ___ ” _____ 20__ р.

З А В Д А Н Н Я**НА ДИПЛОМНУ РОБОТУ СТУДЕНТУ**

Водянику Богдану Романовичу

(прізвище, ім'я, по батькові)

1. Тема роботи Аналіз електроенцефалограм людини, отриманих під час емоційних стимулів

керівник роботи доц. каф. ЕІ, доц., к.т.н. А.О. Попов,

(прізвище, ім'я, по батькові, науковий ступінь, вчене звання)

затверджені наказом по університету від 24 травня 2021 року № 1316-с

2. Строк подання студентом роботи 15.06.2021
3. Вихідні дані до роботи База даних електроенцефалограм, отриманих під час візуальних емоційних стимулів

4. Зміст дипломної роботи (перелік питань, які потрібно розробити)

Теоретичне визначення походження електричного сигналу головного мозку; розгляд пристроїв для реєстрації сигналів ЕЕГ; вивчення основних методів аналізу сигналів ЕЕГ; проведення численного експериментального дослідження реальних ЕЕГ, викликаних емоційнонавантаженими візуальними стимулами.

5. Перелік графічного (ілюстративного) матеріалу (із зазначенням обов'язкових креслень, плакатів, презентацій тощо)






Рисунки в тексті пояснювальної записки, ілюстрації до захисту.

6. Консультанти розділів роботи

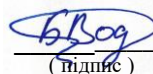
Розділ	Прізвище, ініціали та посада консультанта	Підпис, дата	
		завдання видав	завдання прийняв

7. Дата видачі завдання 01.09.2020

КАЛЕНДАРНИЙ ПЛАН

№ з/п	Назва етапів виконання дипломної роботи	Строк виконання етапів роботи	Примітка
1	Ознайомлення та вивчення природи походження ЕЕГ	01.09.20 – 01.11.20	
2	Дослідження способів реєстрації ЕЕГ	01.11.20 – 01.01.21	
3	Вивчення основних методів аналізу електричних сигналів головного мозку	01.01.21 – 01.03.21	
4	Практична реалізація математичних методів аналізу до реальної бази даних ЕЕГ	01.03.21 – 20.05.21	
5	Оформлення роботи та підготовка до захисту	20.05.21 – 15.06.21	

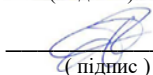
Студент


(підпис)

Водяник Б.Р.

(прізвище та ініціали)

Керівник роботи


(підпис)

Попов А.О.

(прізвище та ініціали)

РЕФЕРАТ

Дипломна робота: 71 с., 4 ч., 1 табл., 34 рис., 44 джерела.

ЕЛЕКТРОЕНЦЕФАЛОГРАМА, ОБРОБКА БІОМЕДИЧНИХ СИГНАЛІВ, АНАЛІЗ СИГНАЛІВ, СПЕКТРАЛЬНИЙ АНАЛІЗ, ПЕРЕТВОРЕННЯ ФУР'Є, РЕЄСТРАЦІЯ БЕГ, ПРОГРАМУВАННЯ PYTHON, СПЕКТРАЛЬНА ПОТУЖНІСТЬ, ДЕТРЕНДОВИЙ АНАЛІЗ КОЛИВАНЬ

Об'єктом розгляду є електрична активність головного мозку людини. Предмет роботи – методи аналізу електроенцефалограм під час дії різноманітних стимулів.

Метою роботи є вивчення природи виникнення електричних сигналів мозку, методи їх реєстрації та аналізу для дослідження реакції на візуальні емоційнонавантажені стимули.

У першому розділі описуються загальні поняття про природу виникнення електричного сигналу мозку людини, а також нейрофізіологічні ознаки присутності різних частотних складових сигналу за певних станів людини.

У другому розділі наведено принципи реєстрації сигналів електроенцефалограми (ЕЕГ) та описано пристрої, що здатні це виконувати. Також розглянуто опис основної системи накладання сенсорів (електродів) на голову людини. В кінці розділу наведено приклад компактного 8-канального енцефалографа власної розробки, що здатен реєструвати сигнали ЕЕГ та передавати їх по бездротовому зв'язку на мобільні прилади (смартфон, планшет).

Третій розділ описує основні математичні методи аналізу ЕЕГ сигналів. Основними є методи спектрального та вейвлет-аналізу та аналіз детрендових коливань, за допомогою яких можна отримати детальне представлення про роботу мозку, шляхом виявлення різноманітних патернів в частотних діапазонах.

У четвертому розділі описується практичне застосування методів спектрального та Detrended Moving Average аналізів на експериментальній базі

даних ЕЕГ для 48 здорових волонтерів, запис ЕЕГ для яких проводився під час демонстрації певних емоційнонавантажених візуальних стимулів. Також в цьому розділі наведені результати виконаного аналізу разом з їх нейрофізіологічним тлумаченням.

ABSTRACT

Diploma project: 71 p., 4 p., 1 table, 34 figures, 44 references.

ELECTROENCEPHALOGRAM, BIOMEDICAL SIGNAL PROCESSING, SIGNAL ANALYSIS, SPECTRAL ANALYSIS, FOURIER TRANSFORM, EEG REGISTRATION, PYTHON PROGRAMMING, SPECTRAL POWER, DFA, DMA

An important place in the study of brain activity is occupied by the study of its electrical potentials. Electroencephalography (EEG) is a method of graphical recording of brain biopotentials, which allows analyzing its physiological maturity and condition, the presence of focal lesions, general brain disorders and their nature. It consists of recording and analyzing the total bioelectric activity of the brain — an electroencephalogram (EEG). EEG can be taken from the scalp, from the surface of the brain, as well as from deep brain structures. As a rule, an electroencephalogram is understood as a surface recording, that is, made from the intact head surface.

EEG is most often used to diagnose epilepsy, which causes EEG disorders. It is also used to diagnose sleep disorders, deep anesthesia, coma, encephalopathy, and brain death. EEG was used as the main method for diagnosing tumors, stroke, and other focal brain diseases, but when it became possible to obtain high-resolution anatomical images using magnetic resonance imaging (MRI) and computed tomography (CT) techniques, the use of EEG declined. Despite its limited resolution, the EEG continues to be a valuable tool for research and diagnosis.

The object of consideration is the electrical activity of the human brain. The subject of the work is methods of analyzing electroencephalograms during the action of various stimuli. The aim of the work is to study the nature of the occurrence of electrical signals of the brain, methods of their registration and analysis to study the response to visual emotional stimuli.

The first chapter describes general concepts about the nature of the occurrence of an electrical signal in the human brain, as well as neurophysiological signs of the presence of various frequency components of the signal in certain human states.

The second chapter describes the principles of recording electroencephalogram signals and describes devices that can perform this. The description of the main system for applying sensors (electrodes) to the human head is also considered. At the end of the section, an example of a compact 8-channel encephalograph of our own design is given, which is able to register EEG signals and transmit them wirelessly to mobile devices (smartphone, tablet).

The third section describes the basic mathematical methods for analyzing EEG signals. The main methods are spectral and wavelet analysis and detrended oscillation analysis, which can be used to get a detailed picture of brain function by identifying various patterns in frequency ranges.

The fourth section describes the practical application of spectral and Detrended Moving Average analysis methods on an experimental EEG database. Here, initially the EEG records were made for 48 healthy volunteers whose EEG recording was performed while demonstrating certain emotionally loaded visual stimuli. Stimuli were selected from the International Affective Pictures System (IAPS) based on their average emotional valence values. In order to assess the induced changes of the brain's electrical activity, the EEG-bands were subdivided in a following way: θ_1 [3.5, 5.8], θ_2 [5.9, 7.4], α_1 [7.5, 9.4], α_2 [9.5, 10.7], α_3 [10.8, 13.5], β_1 [13.6, 25], β_2 [25.1, 40] Hz.

As a result, Power Spectral Density (PSD) were visualized as a map on the schematic figure of the head used to render the statistical significance test, demonstrating that variations in powers for our signals were caused by non-identical forms of visual effect rather than being an accident. These details were also shown in the heads charts.

The study of changes in power spectrum density showed neurodynamics triggered by visual stimulation experience. However, when comparing PSD values obtained during the presentation of the first and second neutral series, it was discovered that when processing neutral images followed by negative stimuli, a well-defined activation focus developed in the left parietal region of the cortex in the θ_2 subband.

The DMA algorithm revealed statistically important variations in the left temporal and frontal regions of the cortex, which were marked by more pronounced activation

during the perception of neutral faces in the presence of positive images. This may be the start of a new path of improved inner focus and meaningful emotional experiences.

As a result, the sex-related aspects of the emotional valence effect on neutral face perception were discovered by analyzing EEG-based brain neurodynamics in the mechanism in perception in human faces of various modalities. The stimulation of two large cognitive networks in the brain: mental or theta-network and cognitive beta-network, was the key distinction.

CONTENT

INTRODUCTION	11
1 BRAIN ACTIVITY AND ITS FEATURES	13
1.1 Lobes of human brain.....	13
1.2 EEG generation	15
1.3 Rhythms of brain activity.....	18
1.4 Conclusions for Chapter 1.....	23
2 RECORDING OF EEG SIGNAL AND ITS MEASUREMENT.....	24
2.1 General Principles of EEG Recording	24
2.2 EEG Device and Its Characteristics	25
2.3 EEG Electrodes Placement on the Human Head	27
2.4 Multichannel EEG Signals Recorder	29
2.5 Conclusions for Chapter 2.....	40
3 METHODS OF EEG SIGNAL PROCESSING	41
3.1 Artefacts of EEG and Independent Component Analysis (ICA).....	41
3.2 Fast Fourier Transform (FFT) Method	45
3.3 Short-time Fourier Transform (STFT) Method	46
3.4 Wavelet transform.....	48
3.5 Detrended fluctuation analysis (DFA).....	50
3.5.1 Detrending moving average (DMA) algorithm	53
3.6 Conclusions for Chapter 3.....	55
4 ANALYSIS OF BRAIN REACTION TO EMOTIONAL FACES	56
4.1 Subjects and data collection	56

	10
4.2 Experiment design.....	57
4.3 Methods used for analysis of brain activity	58
4.3.1 Power spectral density estimation.....	58
4.3.2 Detrended moving average analysis	58
4.3.3 Statistical significance evaluation.....	59
4.4 Experiment results.....	59
4.5 Conclusions for Chapter 4.....	63
CONCLUSIONS	64
REFERENCES	67

INTRODUCTION

Human brain plays the main part in all processes in the body. Signals that appear in it control all functions and general states of our organism. Therefore, understanding of neural features and neurophysiological properties is extremely important as well as methods of its registration and analysis.

Electroencephalography (EEG) is an electrophysiological method of registration and monitoring electrical activity of the human brain on the scalp skin. Here special electrodes are used, that are situated on the scalp noninvasively. The EEG signals are the measurement of currents of neural impulses in the cerebral cortex that appear as a result of activation of brain cells (neurons) by the generating signals inside the dendrites. Particularly these currents are caught by sensors (electrodes) of electroencephalograph.

Investigation of cognitive processes inside the brain can be done by analyzing EEG signals during different irritations. All kinds of human activities such as eye movement, lip movement, remembrance, attention, hand clenching etc., can be detected on visualized EEG signals. These abovementioned states are closely connected with particular frequency bands that help to understand main trends in human's brain activity. So, EEG is a highly efficient method that acquires and shows consequences of changes in the brain states. For analysis the raw EEG signal that has been extracted will be preprocessed that includes acquisition of signal, removal of artifacts, signal averaging, threshold value of the output, enhancement of the resulting signal, and edge detection. The next step is a feature extraction algorithm where the most important features are chosen for further classification. The signal will then be categorized using linear, nonlinear, adaptive, clustering, and fuzzy approaches, as well as neural networks.

In this work, the main principles and definitions of brain activity were described as well as design of registration and analysis of EEG signals. All these things were used to work with real experimental data. The focus here is on the study of electroencephalographic data gathered throughout the experiment, which are designed to specific states of brain activity during various forms of emotional visual stimuli. EEG

data was received from the group of 48 healthy volunteers to which special images with emotional load were shown. In this case for analysis Power Spectral Density (PSD) and Detrended Moving Average (DMA) analysis methods were used. Additionally, to provide the accuracy and relevance of results the statistical significance evaluation was applied.

1 BRAIN ACTIVITY AND ITS FEATURES

1.1 Lobes of human brain

The brain is the most essential functioning organ of our body, it regulates and directs all of our muscles and nerves. The brain is split into two hemispheres, the left and right hemispheres [1]. Each hemisphere is divided into four lobes: Frontal, Temporal, Parietal, and Occipital. The Frontal lobe, which is situated below the forehead, is the main lobe. Speech and expression are regulated by the left Frontal lobe. Planning, scheduling, problem solving, recall, self-regulation, decision making, selective focus, and managing actions and emotions are all topics included in this course. As the frontal lobe is damaged, it may have an impact on feelings, speech and memory.

The temporal lobe is situated on the sides of the brain, behind the Frontal lobe and under the Parietal lobe. This is the part of the brain that controls sound and voice recognition in different forms of memory. During the injury, it can cause hearing, language, and sensory issues [2]. The Occipital lobe is located at the back of the head and is responsible for sensory vision and processing. When the Parietal lobe, which is situated behind the frontal lobe and absorbs sensory input from various areas of the body, is injured, it causes vision and perception problems. It may result in an inability to identify and classify body parts (Figure 1.2).

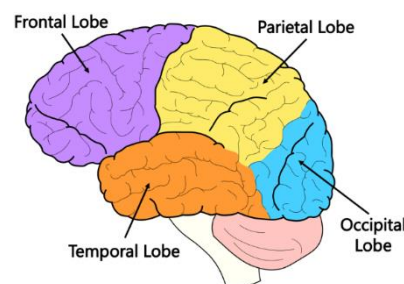


Figure 1.2 – Structure of human brain and its lobes

From the medical history, it is well known that specific action/activity/states are controlled by particular part of the brain. For example, Table 1.1 represents cranial nerve

and its associative functionalities [3]. Electrode locations for EEG recordings are determined by the functional activity of the brain and its corresponding site.

Table 1.1 – Functions of Cranial nerves

№	Name	Function
1	Olfactory	Smell
2	Optic	Vision
3	Oculomotor	Eye movement
4	Trochlear	Eye movement
5	Trigeminal	Facial sensation
6	Abducent	Eye movement
7	Facial	Face movement
8	Vestibulocochlear	Hearing and balance
9	Glossopharyngeal	Taste
10	Vagus	Involuntary muscles
11	Accessory	Voluntary neckmuscle
12	Hypoglossal	Tongue movement

1.2 EEG generation

Electrical dipoles between the soma (body of a neuron) and apical dendrites, which branch from neurons, are produced by combined postsynaptic graded potentials from pyramidal cells, generating electrical potential differences (Figure 1.3). The positive ions of sodium, Na^+ , potassium, K^+ , calcium, Ca^{++} , and the negative ion of chlorine, Cl^- , are pumped through the neuron membranes in the direction controlled by the membrane potential to produce current in the brain [4].

The human head is made up of many layers, including the hair, skull, brain (Figure 1.4), and several thin layers in between. The impulses are attenuated one hundred times more from the brain than by soft tissue. The majority of noise, on the other hand, is produced either inside the brain (internal noise) or over the scalp (external noise) (system noise or external noise). As a result, only broad numbers of active neurons can produce enough potential for the scalp electrodes to register. These signals are later amplified greatly for display purposes. When the central nervous system (CNS) is full and functioning, approximately 10^{11} neurons are created [2]. This equates to 10^4 neurons per cubic mm on average. Synapses connect neurons together to form neural networks. Synapses are found in about 5×10^{14} synapses for adults. With age, the amount of synapses per neuron rises, although the number of neurons declines. The cerebrum, cerebellum, and brain stem are the three portions of the brain that may be separated anatomically. The cerebral cortex is made up of deeply convoluted surface layers that cover both the left and right lobes of the brain.

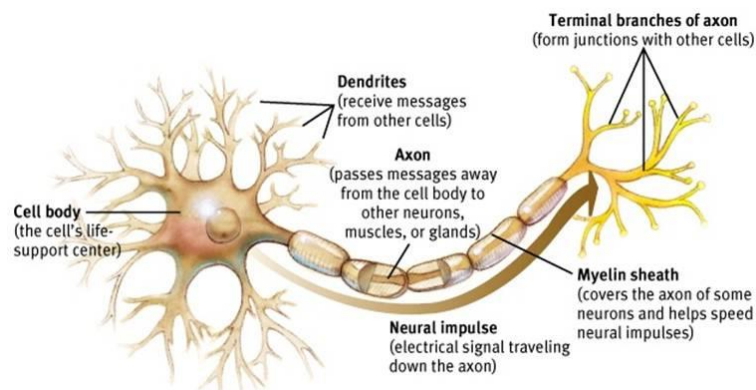


Figure 1.3 – Structure of a neuron

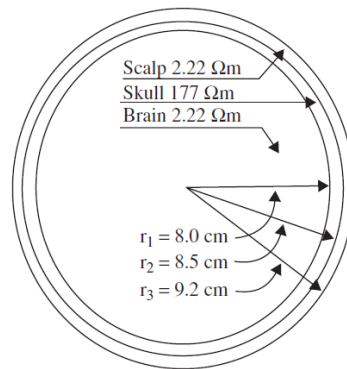


Figure 1.4 – The three main layers of the brain including their approximate resistivities and thicknesses ($\Omega = \text{ohm}$)

Movement initiation, cognitive perception of sensation, complex interpretation, and emotional and behavioral processing all take place in the cerebrum. The cerebellum preserves equilibrium by coordinating voluntary muscle motions. Respiration, pulse regulation, biorhythms, and neurohormone and hormone parts are all regulated by the brain stem [5].

EEG research clearly paves the way for the detection of a wide range of brain diseases and other anomalies in the human body. The EEG signs obtained from a person (and even from animals) can be used to investigate the following clinical problems [5, 2]

1. monitoring the brain development;
2. controlling anaesthesia depth (servo anaesthesia);
3. testing afferent pathways (by evoked potentials);
4. investigating mental disorders;
5. assisting in experimental cortical excision of epileptic focus;
6. locating areas of damage following head injury, stroke, and tumour;
7. investigating epilepsy and locating seizure origin;
8. effects testing drugs for convulsive effects;
9. providing a hybrid data recording system together with other imaging modalities;
10. monitoring alertness, coma, and brain death;
11. testing epilepsy drug;

12. investigating sleep disorders and physiology;
13. monitoring cognitive engagement (alpha rhythm);
14. producing biofeedback situations.

This list confirms the rich potential for EEG analysis and motivates the need for advanced signal processing techniques to aid the clinician in their interpretation.

1.3 Rhythms of brain activity

Visual inspection of EEG signs may be used to detect a variety of neurological problems. The appearance of brain patterns in EEG signals is well-known by scientific specialists in the area. The amplitudes and rhythms of certain signals shift in healthy adults when they transition from one stage to another, such as wakefulness and sleep. Over age, the properties of the waves shift as well. The varying frequency ranges of the five main brain waves differentiate them. These frequency bands from low to high frequencies respectively are called alpha (α), theta (θ), beta (β), delta (δ), and gamma (γ). The alpha and beta waves were introduced by Berger in 1929. Jasper and Andrews (1938) used the term ‘gamma’ to refer to the waves of above 30 Hz. The delta rhythm was introduced by Walter (1936) to designate all frequencies below the alpha range. He also introduced theta waves as those having frequencies within the range of 4–7.5 Hz. The notion of a theta wave was introduced by Wolter and Dovey (1944) [6].

Delta waves (Figure 1.5) lie within the range of 0.5–4 Hz. These waves are most often correlated with deep sleep, but they can also be seen in the waking state. It's possible to confuse artefact messages from the big muscles of the neck and jaw with the real delta reaction. This is due to the fact that muscles emit massive signals near the skin's surface, while the signal of importance originates deep inside the brain and is severely attenuated when it passes across the skull. However, it is very straightforward to see whether a reaction is triggered by unnecessary activity by implementing basic signal analysis methods to the EEG.

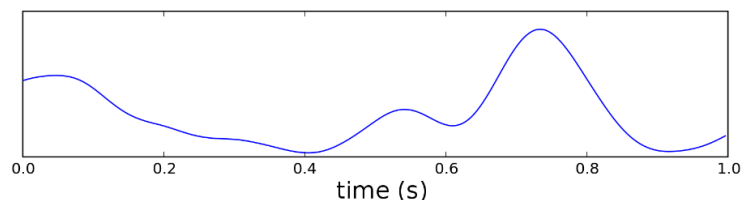


Figure 1.5 – Delta waves

Theta waves (Figure 1.6) lie within the range of 4–7.5 Hz. It's possible that term theta was selected to allude to its thalamic roots. When awareness begins to lapse into

drowsiness, theta waves emerge. Access to unconscious content, artistic motivation, and deep reflection have all been linked to theta waves. A theta wave is often followed by other frequencies and seems to be linked to arousal levels. Healers and experienced mediators are believed to have an alpha wave that steadily decreases in magnitude over time. Infancy and adolescence, the theta wave is quite significant. In the waking human, larger contingents of theta wave activation are rare and are triggered by a variety of pathological issues. Theta wave pattern variations was investigated for maturational and emotional research [2].

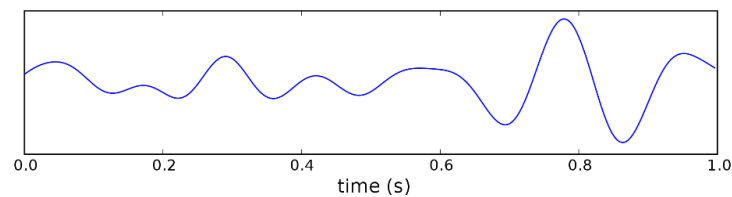


Figure 1.6 – Theta waves

Alpha waves (Figure 1.7) appear in the posterior half of the head and are usually found over the occipital region of the brain. They can be found in all areas of the brain's posterior lobes. The frequency of alpha waves is between 8 and 13 Hz, and they usually behave as a circular or sinusoidal formed signal. In extreme instances, though, it may manifest as sharp waves. In such cases, the negative component appears to be sharp and the positive component appears to be rounded, similar to the wave morphology of the rolandic mu (μ) rhythm. Alpha waves are considered to represent both a calm consciousness and a lack of focus or concentration. The alpha wave is the most common rhythm of all of brain function, and it can extend across a wider spectrum than commonly thought. In the beta wave spectrum, a peak can be observed on a daily basis at frequencies up to 20 Hz, and has the properties of an alpha wave state rather than a beta wave state. Again, a reaction at 75 Hz, which occurs in an alpha environment, is quite common. With their eyes closed, most people emit any alpha waves, which is why it's been suggested that it's only a waiting or scanning pattern generated by the brain's visual regions. Opening the eyes, experiencing new stimuli, fear, and internal focus or attention all help to mitigate or remove it. Albert Einstein was able to solve complicated mathematical problems when staying in the alpha state, including the presence of beta and theta waves. An alpha wave

has a higher amplitude over the occipital areas and has an amplitude of normally less than $50 \mu\text{V}$. An alpha wave's genesis and physiological importance are unclear, and further study is needed to understand how this phenomenon emerges from cortical cells.

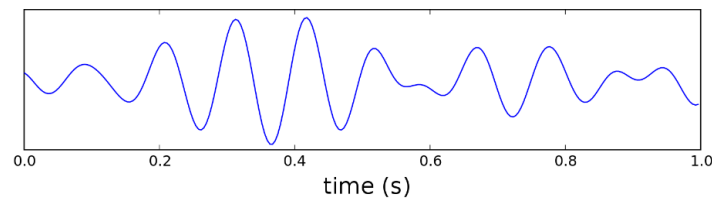


Figure 1.7 – Alpha waves

A *beta wave* (Figure 1.8) is the electrical activity of the brain varying within the range of 14–26 Hz (though in some literature no upper bound is given). Normal people have a beta pulse, which is the brain's normal waking cycle synonymous with active thought, active interest, concentration on the outer environment, or solving concrete issues. When an individual is in a panic condition, a high-level beta wave may be detected. The frontal and central regions of the brain display a lot of rhythmical beta action. A central beta rhythm is linked to the rolandic mu rhythm, and it can be disrupted by motor movement or tactile stimuli. The amplitude of beta rhythm is normally under $30 \mu\text{V}$. Similar to the mu rhythm, the beta wave may also be enhanced because of a bone defect and also around tumoural regions [7].

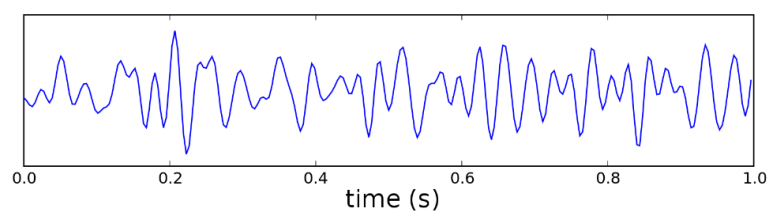


Figure 1.8 – Beta waves

The frequencies above 30 Hz (mainly up to 45 Hz) correspond to the *gamma waves* (sometimes called the fast beta wave). Detection of these rhythms may be used to confirm the presence of some brain conditions, despite the fact that their amplitudes are very limited and their frequency is uncommon. The frontocentral field contains elevated EEG frequencies and the maximum rate of cortical blood supply (as well as oxygen and glucose uptake). The gamma wave band has also been demonstrated to be a good predictor of

event-related synchronization (ERS) in the brain, and it can be used to show the locus for right and left index finger activity, right toes, and the very general and bilateral region for tongue movement [2].

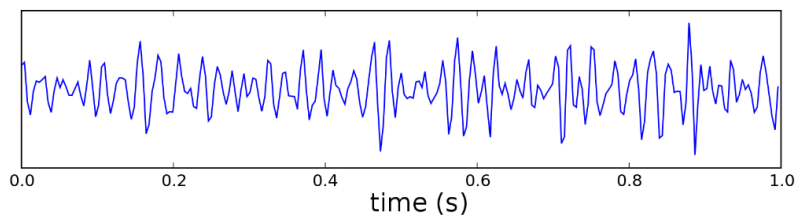


Figure 1.9 – Gamma waves

Waves with frequencies significantly higher than the EEG's usual activity range, typically in the 200–300 Hz range, have been discovered in animal cerebellar regions, although they have not been linked to clinical neurophysiology [7].

Figure 1.10 shows the typical normal brain rhythms with their usual amplitude levels. In general, the EEG signals are the projection of neural activities that are attenuated by leptomeninges, cerebrospinal fluid, dura matter, bone, galea, and the scalp. Cartographic discharges show amplitudes of 0.5–1.5 mV and up to several millivolts for spikes. However, on the scalp the amplitudes commonly lie within 10–100 μV .

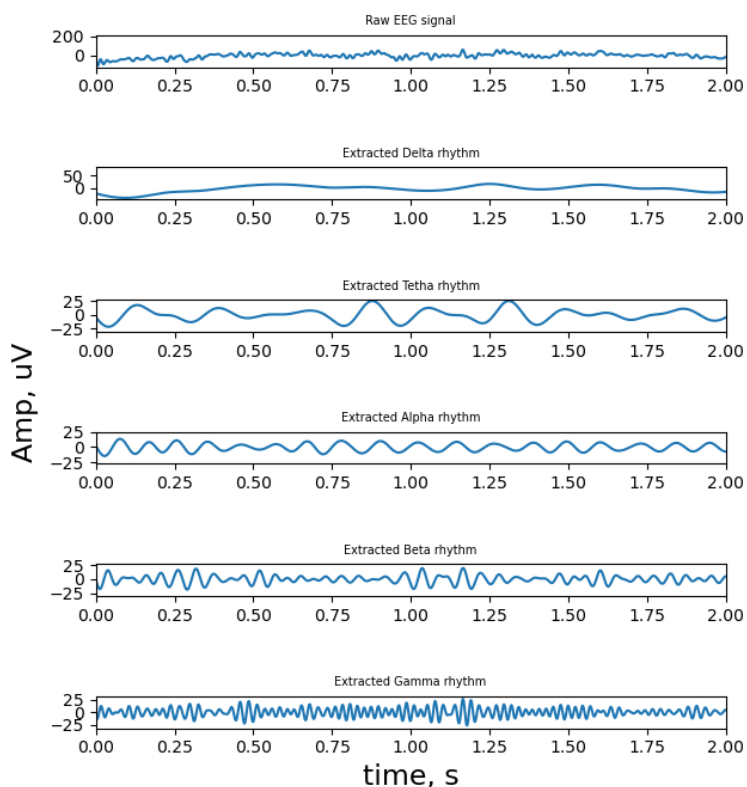


Figure 1.10 – Raw EEG signal and the extractions of signal

The above rhythms will last for a long time if the subject's condition does not shift, because they are roughly cyclic in nature. On the other hand, there are other brain waveforms, which may:

- Have a wide frequency range or appear as spiky-type signals, such as K-complexes, vertex waves (which occur during sleep), or a breach rhythm, which is an alpha-type rhythm that is observed predominantly over the midtemporal region (under electrodes T3 or T4), as well as some seizure signals.
- Be a transient such as an event-related potential (ERP) and contain positive occipital sharp transient (POST) signals (also called rho (ρ) waves).
- They come from defective areas of the brain, such as tumoral brain lesions.
- Be spatially localized and cyclic in nature, but be quickly disrupted by bodily movement, such as the mu rhythm. Mu stands for motor and is closely linked to the motor cortex. In terms of amplitude and frequency, Rolandic (central) mu is similar to posterior alpha. The topography and physiological relevance, on the other hand, are substantially different. The mu rhythm may be used to explore cortical functioning and variations in brain (mainly bilateral) activity in response to actual and virtual motions. The mu rhythm has also been employed in feedback training for a variety of applications, including epileptic seizure condition therapy [6].

Also with educated eyes, it may be hard to recognize and sense brain patterns from scalp EEGs. Advanced signal processing equipment, on the other hand, should be able to separate and analyze the target waveforms from inside the EEGs. As a result, defining foreground and background EEG is highly arbitrary and highly dependent on abnormalities and applications [7].

1.4 Conclusions for Chapter 1

For those who work with signals for the identification, evaluation, and treatment of brain abnormalities and diseases, a thorough understanding of neuronal functions and neurophysiological properties of the brain, as well as the processes influencing signal generation and processing, is essential. EEG signals are the electrical ones that appear as a result of activation of brain cells.

Analysis of EEG rhythms gives the description of the human's brain state, because each frequency band is connected with a particular kind of activity. So, using different methods of extraction of signals for special bands we can provide all necessary information for understanding processes in the brain.

2 RECORDING OF EEG SIGNAL AND ITS MEASUREMENT

2.1 General Principles of EEG Recording

Simple galvanometers were used to record the first electrical neural processes. To amplify extremely fine fluctuations in the pointer, a mirror was employed to reflect the light reflected to the galvanometer on the wall. A mirror placed on a moveable coil was subsequently added to the d'Arsonval galvanometer, and light focused on the mirror was reflected when a current went through the coil. Lippmann and Marey [8] invented the capillary electrometer. Einthoven created the string galvanometer in 1903 as a more sensitive and precise measurement tool. For a few decades, this was a common tool that allowed for photographic recording.

A variety of delicate electrodes, a series of differential amplifiers (one for each channel), filters, and needle (pen)-type registers make up more recent EEG systems. The multichannel EEGs could be graphed on either plane or grid paper. Researchers began searching for a computerized device that could digitize and store signals soon after this system was introduced to the market. As a result, it was quickly realized that EEG signals must be in digital form in order to be analyzed. This necessitated signal sampling, quantization, and encoding. When the number of electrodes rises, so does the data amount in terms of bits. Variable configurations, stimulations, and sampling frequency are possible for computerized devices, and others are fitted with basic or specialized signal processing tools for signal processing.

The conversion from analogue to digital EEG is performed by means of multichannel analogue-to-digital converters (ADCs). Fortunately, EEG signals have a restricted effective bandwidth of around 100 Hz. This bandwidth may be regarded even half of this figure for many applications. As a result, sampling the EEG signals at a minimum frequency of 200 samples/s (to meet the Nyquist criteria) is sufficient. Sampling frequencies of up to 2000 sample/s may be employed in certain situations where a greater resolution is needed for depiction of brain processes in the frequency domain [7].

2.2 EEG Device and Its Characteristics

Electroencephalography is a technique that reads electrical potential from the brain and measured using special device called Electroencephalogram (EEG). This device comprised of electrodes, conductive gel, amplifiers and Analog to Digital converter as shown in Figure 2.1. The electrodes or leads are used to conduct electrical activity from the scalp of the brain. Different types of electrodes are used in general for EEG analysis [3].

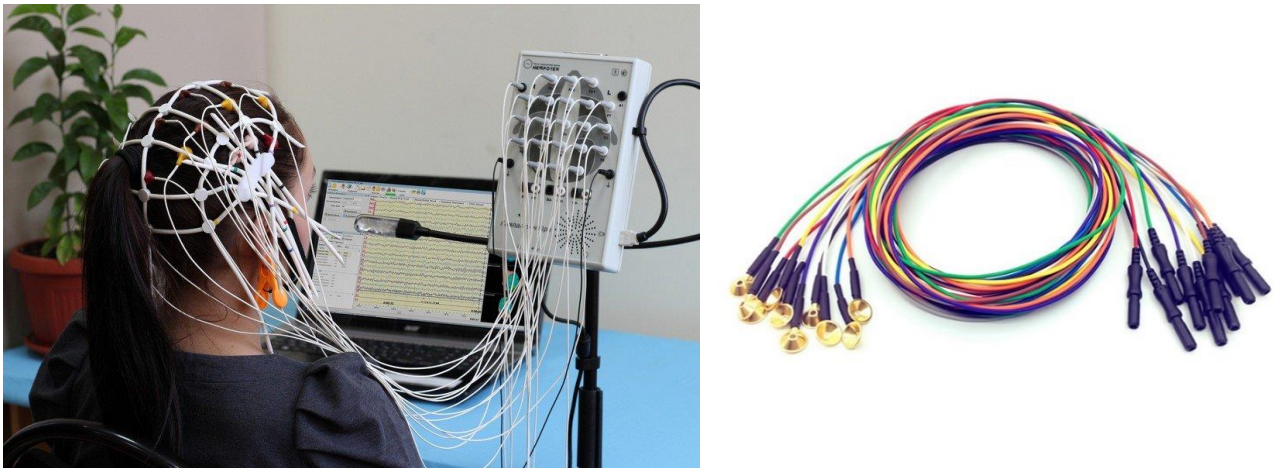


Figure 2.1 – (a) Electroencephalograph; (b) Electrodes for EEG recording

The EEG recording electrodes and their proper function are crucial for acquiring high-quality data. Different types of electrodes are often used in the EEG recording systems, such as [7]:

- disposable (gel-less, and pre-gelled types);
- saline-based electrodes;
- needle electrodes;
- reusable disc electrodes (gold, silver, stainless steel, or tin);
- headbands and electrode caps.

Electrode caps are often used in multichannel recordings with a high number of electrodes. Commonly used scalp electrodes consist of Ag–AgCl disks, less than 3 mm in diameter, with long flexible leads that can be plugged into an amplifier. These

electrodes placed on the scalp with small amount of conductive gel (Ag-Cl) applied under the disk. Disk will be with gold, tin and silver compositions. The cost of the electrode is low and life may depend upon metal used on disk and insulating medium on wire. These electrodes have chance to fall down from the scalp which leads higher chances of artifacts [9]. EEG cap is another type, which allows you to choose various numbers and sizes of electrodes. EEG caps are also available for reusable disks that are injected with conductive gel into the cap's openings. It is recommended for multi-channel capture, but one problem with this cap is that if one electrode fails, the whole cap must be replaced, and it is impossible to track down the failed electrode [3].

High impedance between the brain and the electrodes, as well as high impedance electrodes, may cause distortion and even obscure the EEG signals. Impedance monitors are often included in commercial EEG recording systems. The electrode impedances should be less than 5 kOhm and balanced to within 1 kOhm of each other for a decent recording. The impedances are tested after each trial for more precise measurement. The distribution of potentials across the scalp (or cortex) is not uniform due to the layered and spiral structure of the brain. Some of the findings of source localisation utilizing EEG signals may be affected as a consequence of this [7].

2.3 EEG Electrodes Placement on the Human Head

The typical electrode setting (also known as 10–20) for 21 electrodes (excluding the earlobe electrodes) is suggested by the International Federation of Societies for Electroencephalography and Clinical Neurophysiology, as shown in Figure 2.2. The reference electrodes are often the earlobe electrodes A1 and A2, which are linked to the left and right earlobes, respectively. The 10–20 approach eliminates eyeball placement and takes into account certain fixed lengths by measuring particular anatomic features and then utilizing 10 or 20% of that distance as the electrode spacing. On the left are the odd electrodes, while on the right are the even electrodes.

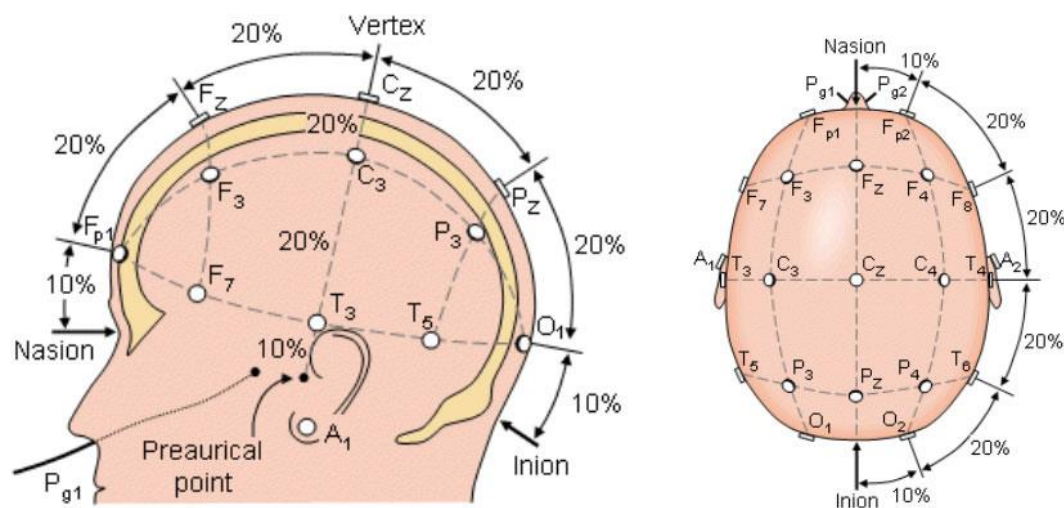


Figure 2.2 – Point labels of 10-20 electrode placement system

For setting a larger number of electrodes using the above conventional system, the rest of the electrodes are placed in between the above electrodes with equidistance between them. For example, C1 is placed between C3 and Cz. Extra electrodes are sometimes used for the measurement of EOG, ECG, and EMG of the eyelid and eye surrounding muscles [7].

The electrodes are arranged according to 10-20 standards for EEG placement. These electrodes are labeled by letters (F-Frontal, T-Temporal, C-Central, P-Parietal) which indicates the lobes of the brain. Midline region is referred by a label with 'z'. Odd

numbers indicate left hemisphere and even numbers are used to indicate right hemisphere. For example, C3 is located on left central lobe. An additional sensor is used to record special applications such as, heart rate, skin conductance, eye movements, and respiration.

EEG atlas with respect to electrode position is given the Figure. 3. Cortex around Cz, C3 and C4 locations deals with sensory and motor functions. Pz, P3 and P4 are related to cognitive processing. T4 and T6 represent emotional memory while T3 and T5 stands for verbal memory functions. Oz, O1 and O2 deals with visual processing stimuli. Fz is placed near intentional and motivational centers, F8 and F7 are located close to emotional and verbal expressions. F3 and F4 are located at motor planning activities. Fpz, Fp1 and Fp2 deals with attention and judgment impulses [3].

The placement of electrodes, also known as Montages, is done in one of two ways: Referential or Bipolar electrodes. The potential difference between each electrode and the reference electrode is recorded in the Referential process. When setting the reference electrode on the tip of the nose or the base of the foot, it is not ideal. Related ear refers to the placement of reference electrodes on both ear lobes. Potential variations between paired active electrodes are reported in the bipolar system. It binds the electrodes in a logical order, forming a Longitudinal or Transverse form [10].

2.4 Multichannel EEG Signals Recorder

There are more than a few articles that describe the developed prototypes of EEG recording systems. In [11], a computationally powerful system with 32 dry active electrodes (based on TLC272 precision OP) for long-term monitoring of an epileptic patient is presented. The battery-powered design featured a 24-bit resolution of the ADS1299 analog-to-digital converter. EEG data can be processed in real time on a dedicated ARM processor with a frequency of 1 GHz or transmitted to the host computer via Wi-Fi for analysis and further processing. Although the main purpose of the work was to create a stand-alone system with a more productive processor, the maximum battery life of 25 hours was the main limitation when working under maximum load. Because the device was not optimized in size, it required longer wires and the use of active electrodes.

A similar approach was used in [12]. When developing its EEG collection system to solve the problem of monitoring the steady state of visually evoked potentials (SSVEP). The 16-channel Beagle Bone Black device (based on the AM3358 ARM Cortex-A8 1 GHz processor) was developed with two ADS1299 ADCs and is capable of sampling at 1 ksps. The authors claimed that their system was superior to others due to the built-in computing power and the ability to run up to 12 hours on two lithium batteries.

In [13], an inexpensive 7-channel, small, and battery-powered EEG solution was developed for long-term monitoring of patients with schizophrenia. The board used one ADS1299 ADC controlled by a SAM G55 microcontroller. The authors claimed that their system captures analog data with a sampling rate of 250 Hz and transmits them via Bluetooth. It was reported that the power consumption is 69 mA with all active channels.

Similarly, in [14] presented an inexpensive 8-channel EEG recording device for use in the neurocomputer interface. The device was developed on a STM32F4 microcontroller, one ADS1299 and a Bluetooth module, the design was focused on small size and low power consumption. The sampling rate of 250 Hz was used to record the EEG using wet electrodes with gold cups.

The article [15] presented a tiny 4-channel device that is inserted into the ear. Based on the ideas of the OpenBCI project, the authors developed a BCI board with an ADS1299 ADC, which was connected using an Atmega328 microcontroller. Raw EEG data was sent via Bluetooth to a remote computer host for processing.

The idea of building a compact, cheap, simple and energy efficient device was taken as a basis. The ADS1299 frontend and a microcontroller with modern wireless interfaces and the ability to connect to a desktop computer were chosen as the basis. The recommended sensors are dry cup electrodes, which is one of the most popular solutions. The device itself will record signals from 8 channels. The power source will be one lithium-ion battery, which will provide about 10 hours of active operation.

The decision to build an 8-channel device is based on the fact that it will make the device very compact and versatile. So it can be used for the general scheme of the 8-channel arrangement of electrodes (Figure 2.3).

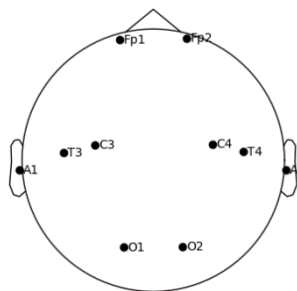


Figure 2.3 – General scheme of 8-channel electrode placement system

This principle allows to locate problem areas and make the first assessment of the patient's condition. In the future, the electrodes can be placed more locally, which will give a complete picture of the state of activity of the brain. This fact is decisive. This will allow the device to be used both for stationary examinations and for use by mobile ambulance crews. The small number of electrodes allows to work with both adults and even babies, as the electrodes can be placed quite neatly and accurately in small areas.

The selected microcontroller will ensure the versatility and simplicity of the device during the software development stages, and wireless interfaces will create all the conditions for easy use of the device in any conditions. The general block diagram that describes the device is presented in Figure 2.4.

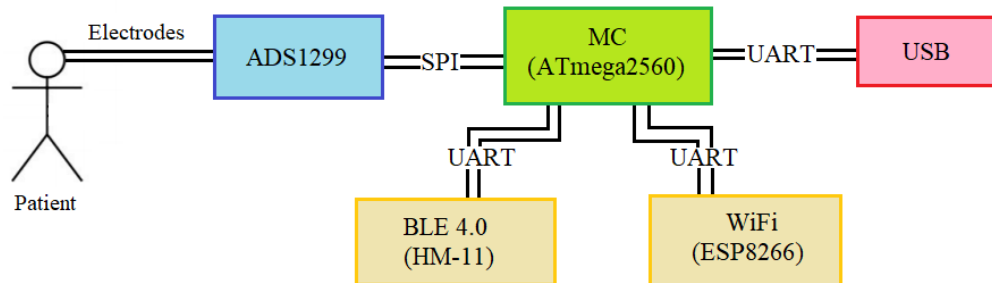


Figure 2.4 – Block diagram of the electroencephalograph

The basis of the EEG recorder is the frontend ADS1299, it provides the required number of channels, noise level, ADC resolution, which are described in the requirements for the project. All the received information is transmitted first to the microcontroller ATmega2560, and then to the periphery of the interfaces.

The ATmega 2560 microcontroller is chosen because of its availability and simplicity. This unit is the central "core" of the famous Arduino Mega board, so there is a large number of ready-made libraries and a developed environment for programming. It is possible also further update the device software with ready-made methods: using a special USBAsp programmer, the connector for which is installed in the recorder.

This EEG recorder has two data interfaces:

- Wi-Fi module (ESP8266-12E)
- Bluetooth module (HM-11)

The above modules provide stable wireless information exchange. The models themselves were chosen for reasons of accessibility and simplicity. Another advantage is that these boards are available ready-made with antennas and the necessary additional components on a solid textolite substrate. This is an outstanding parameter, as it ensures the correct operation of the board, because the introduction of such modules "directly" has many additional design features related to frequency bands, antenna shape and more.

Ready-made modules simplify the design and ensure correct operation, while maintaining its simplicity.

This device also has a USB connector, which transfers information via the CP2102 module, which connects the microcontroller and the USB port.

All of the above interfaces make the EEG recorder quite versatile, providing the ability to analyze brain activity both with a computer and using a smartphone or tablet, connecting via a wireless channel.

To ensure patient safety during the examination and the simultaneous connection of the recorder to the USB port, a galvanic isolation was added to the ADUM2402B board, which will protect the patient from possible breakdowns and surges from the port connected to the computer. This board is quite modern, cheap and simple, retaining all the necessary features.

To ensure correct timing of the frontend and the microcontroller, a quartz oscillator (HC735-2.048MHZ) and a resonator (CSTCE16M0V) were connected to the special outputs, respectively, the operating frequencies of which were selected according to the technical description of the boards (datasheet).

The recorder is powered by a lithium-ion battery NCR18650PF (3.7 V). This choice will provide a fairly long service life and relatively high efficiency, and also makes the device convenient in terms of weight and dimensions, which, of course, will be reflected in the use of the device.

Branching of power supply into two main directions: "analog" and "digital" power supply; was implemented in two blocks. Analog power (5 V) is based on the MT3608 chip, which is very simple, small and extremely cheap. Additional passive elements in this unit were selected according to the existing design of the finished device. The digital power supply (3.3 V) is built on the TPS7A2033 chip, which is already a ready-made voltage reducer, so only protective capacitors have been added here.

The main number of passive elements was taken in accordance with the technical recommendations for each individual board. The calculation was performed separately for the voltage booster unit based on MT3608. According to the technical recommendation [16]:

$$V_{\text{OUT}} = V_{\text{REF}} \times \left(1 + \frac{R_1}{R_2}\right), \text{ de } V_{\text{REF}} = 0,6 \text{ V}$$

$$\frac{R_1}{R_2} = \frac{V_{\text{OUT}}}{V_{\text{REF}}} - 1 = \frac{5}{0,6} - 1 = 7,5$$

$$R_2 = 1 \text{ k}\Omega \rightarrow R_1 = 7,5 \text{ k}\Omega$$

According to the scheme: $R_{18} = 1 \text{ k}\Omega$, $R_{17} = 7,5 \text{ k}\Omega$

Also for part of the DC-DC step up circuit on MT3608 the other part of the passive components is selected according to the technical recommendation for stable operation (Figure 2.5) [17]:

$L1 = 22 \mu\text{H}$, $D1 - \text{SS34}$, $C2 = 22 \mu\text{F}$, $C3 = 22 \mu\text{F}$.

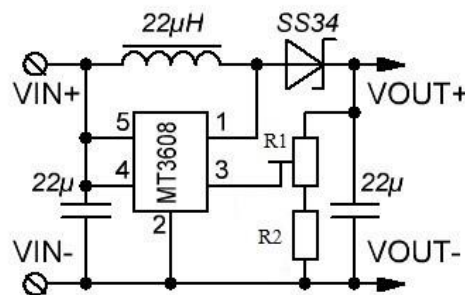


Figure 2.5 – MT3608 connection

To calculate the RC filters at the inputs of the electrode connection, we use the information that the resistance of the electrode is taken $\approx 50 \text{ k}\Omega$, then, based on the information from the description of ADS1299 Demonstration Kit [18], choose the value of the input resistors $5.1 \text{ k}\Omega$. Then according to the set frequency range of measurement (0,1-200 Hz), we have:

$$f = \frac{1}{2\pi RC} \rightarrow C = \frac{1}{2\pi Rf} = \frac{1}{2 \cdot 3,14 \cdot 55 \cdot 10^3 \cdot 200} \approx 13 \text{ (nF)}$$

To provide a certain "margin" in frequency, the nominal capacitors are selected 10 nF .

Therefore, C1, C9-C16 are selected at 10 nF each. Also, according to the demonstration set, a shunt capacitor C21 = 1 μ F was chosen (Figure 2.6).

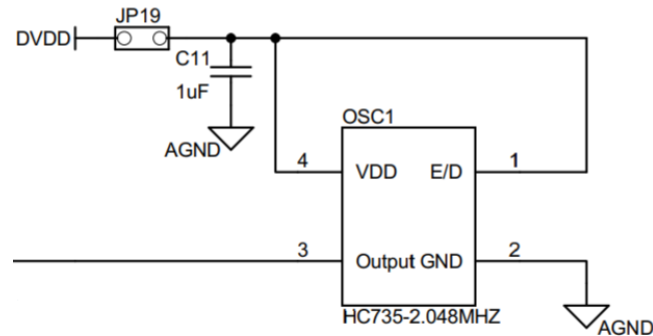


Figure 2.6 – HC735 connection

The nominal values of the components for the 3.3 V digital voltage converter were selected according to the manual for the main component TPS7A2033 (Figure 2.7) [19]: C5 = 1 μ F, C4 = 1 μ F.

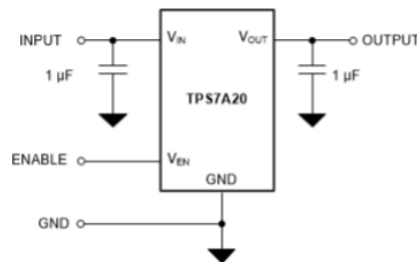


Figure 2.7 – Power connection for TPS7A2033

Capacitor ratings C6 = 1 μ F, C17 = 0.1 μ F, C29 = 10 μ F, C30 = 0.1 μ F, C24 = 1 μ F, C25 = 1 μ F, C26 = 100 μ F, C18 = 1 μ F, C19 = 0.1 μ F, C20 = 0.1 μ F, C27 = 0.1 μ F, C23 = 1 μ F, C22 = 0.1 μ F; were selected according to the unipolar power supply circuit from the technical documentation for ADS1299 (Figure 2.8) [20].

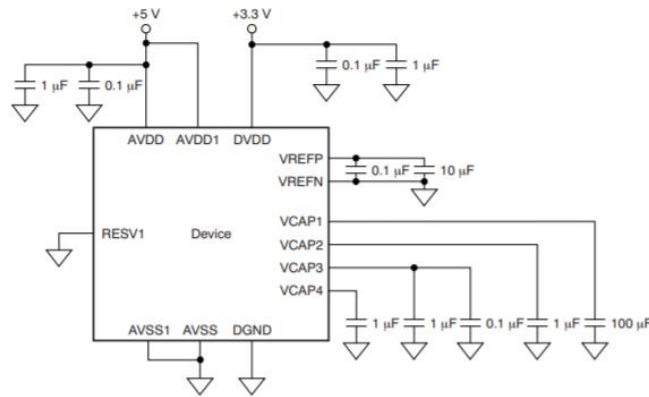


Figure 2.8 – Unipolar power supply circuit for ADS1299

Resistors $R6 = 24 \text{ k}\Omega$, $R7 = 47 \text{ k}\Omega$ are selected from the configuration of the power connection of the board CP2102 (Figure 2.9) [21].

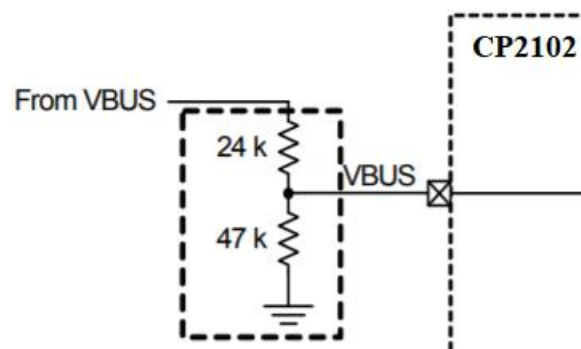


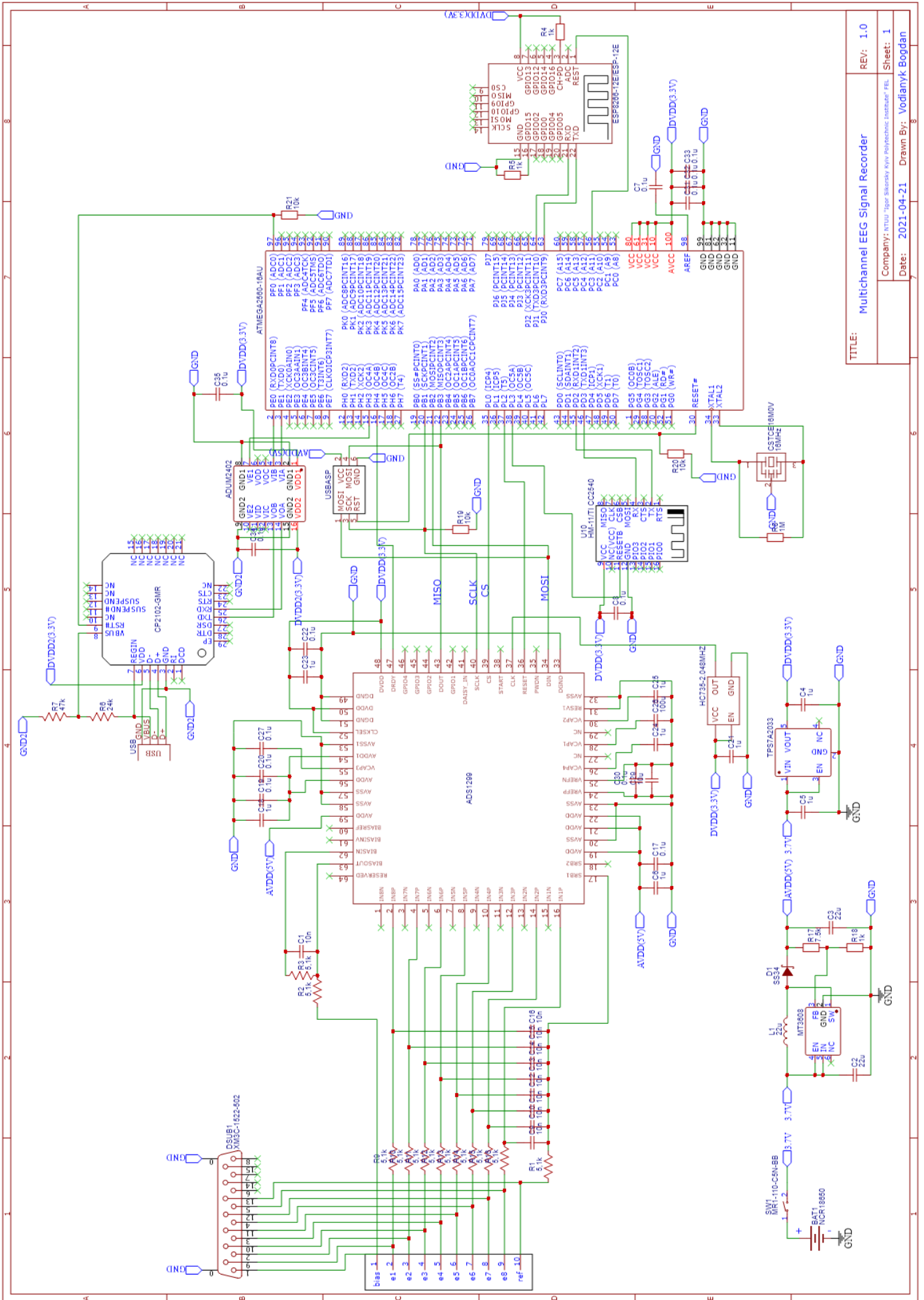
Figure 2.9 – Power supply CP2102

The values of capacitors $C34 = 0.1 \mu\text{F}$, $C35 = 0.1 \mu\text{F}$ are selected from the general information about the power connection with a more correct mode of operation than the direct connection of voltage and ground, without a shunt capacitor.

Resistors $R19 = R20 = R21 = 10 \text{ k}\Omega$ are ground-loop resistors, so the value was chosen according to the basic understanding of their functionality.

The shunt resistor $R8 = 1 \text{ M}\Omega$ is standard for the CSTCE16MOV resonator mounted on the Arduino Mega board (Figure 2.10) [22].

So, in total we have ~ 230mA. The NCR18650PF battery, which has a capacity of 2900mAh, at this load will provide an active mode of operation of about 10-12 hours, taking into account different temperature conditions and the quality of the battery.



TITLE: Multichannel EEG Signal Recorder
REV: 1.0
Company: VTIU - Igor Savitsky 5/16 Polytechnic Institute, FEI
Date: 2021-04-21
Drawn By: Vodiannyk Bogdan
Sheet: 1

Figure 2.12 – Electrical schematic diagram of the 8-channel encephalograph

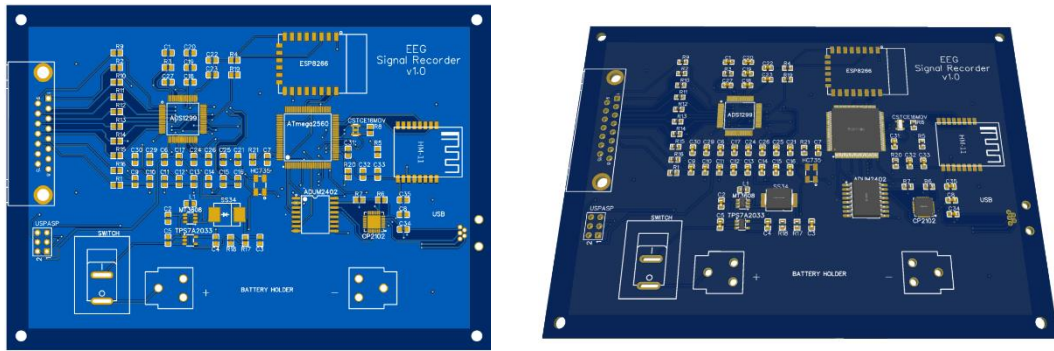


Figure 2.13 – Visualization of the 8-channel encephalograph’s circuit board

The developed device fully corresponds to the task and the chosen concept. The dimensions of the board are 132mm x 94mm. Given the fact that it is already a ready-made device, then, even taking into account the body, the dimensions remain compact. Combined with energy efficiency of up to 10 hours of active operation, this is 70-80 measurements. This result is very good. All these parameters provide good efficiency both in stationary mode for diagnosis and as a portable device for use by doctors in work outside the clinic on the go. Wireless interfaces provide a stable connection to modern mobile devices. The use of the selected microcontroller and a special programming port makes the process of firmware and subsequent software updates quite easy. One can use a ready-made Arduino development environment with all libraries, which is a universal solution, through which the board can be used not only for patient analysis, but also as a training model for research in the direction of analysis of brain activity signals.

2.5 Conclusions for Chapter 2

In this chapter principles of recording EEG signals were shown. To receive electrical signals, the complex of electroencephalograph and a set of special electrodes are used. According to the international system “10-20” all electrodes are put on the scalp skin, each of them makes the recording for one channel. Particularly this placement helps to efficiently detect electrical signals from all regions of the human brain.

Also in this chapter the construction of a compact EEG recorder was shown. Here, there are descriptions of all necessary components that are needed to create an 8-channel EEG recorder. This device can be useful in the sphere of urgent medicine to measure brain activity signals apart from the hospitals, it will help in detecting pathological patterns during patient's transferring.

3 METHODS OF EEG SIGNAL PROCESSING

3.1 Artefacts of EEG and Independent Component Analysis (ICA)

The raw EEG signals will likely be contaminated by undesirable non-cerebral origin signal called artifacts or noises. These artifacts are caused by biological sources and external sources. The existing of the artifacts in EEG signal attenuates the brain originating signal which could lead to misinterpreting the brain activity and misdiagnosis of the brain disorder. Thus, the first step in analyzing EEG signal is to remove the artifacts while enhancing the brain signal. There are several techniques which have been used in separating and removing the artifacts, including notch filter and fixed linear filter. Notch filter is often used to filter the line interference noise in case the data acquisition system of the EEG is unable to cancel out the 50 Hz line frequency. However, the use of filter such as a low - pass filter (LPF) and high-pass filter (HPF) are not advisable since linear filtering could possibly attenuate the brain signals as well, since the frequency band for both artifacts and brain signals could be overlapped. Researchers have developed many techniques for artifact removal, including regression-based methods, component-based methods and adaptive filtering methods [24].

Independent component analysis (ICA) is a computer approach for separating multivariate signals into additive subcomponents in signal processing. This is accomplished by assuming that the subcomponents are non-Gaussian signals that are statistically independent. Blind source separation is a specific instance of ICA. The "cocktail party problem," which involves listening in on one person's conversation in a noisy room, is a frequent example application [25].

Linear independent component analysis can be divided into noiseless and noisy cases, where noiseless ICA is a special case of noisy ICA. Nonlinear ICA should be considered as a separate case [26].

The data are represented by the observed random vector $\mathbf{x} = (x_1, \dots, x_m)^T$ and the hidden components as the random vector $\mathbf{s} = (s_1, \dots, s_n)^T$. The task is to transform the observed data \mathbf{x} , using a linear static transformation \mathbf{W} as $\mathbf{s} = \mathbf{W}\mathbf{x}$, into a vector of

maximally independent components \mathbf{s} measured by some function $F(s_1, \dots, s_n)$ of independence.

Linear noiseless ICA

The components x_i of the observed random vector $\mathbf{x} = (x_1, \dots, x_m)^T$ are generated as a sum of the independent components s_k , $k = 1, \dots, n$:

$$x_i = a_{i,1}s_1 + \dots + a_{i,k}s_k + \dots + a_{i,n}s_n$$

weighted by the mixing weights $a_{i,k}$.

The same generative model can be written in vector form as $\mathbf{x} = \sum_{k=1}^n s_k \mathbf{a}_k$, where the observed random vector \mathbf{x} is represented by the basis vectors $\mathbf{a}_k = (\mathbf{a}_{1,k}, \dots, \mathbf{a}_{m,k})^T$. The basis vectors \mathbf{a}_k form the columns of the mixing matrix $\mathbf{A} = (\mathbf{a}_1, \dots, \mathbf{a}_n)$ and the generative formula can be written as $\mathbf{x} = \mathbf{A}\mathbf{s}$, where $\mathbf{s} = (s_1, \dots, s_n)^T$.

Given the model and realizations $\mathbf{x}_1, \dots, \mathbf{x}_N$ of the random vector \mathbf{x} , the task is to estimate both the mixing matrix \mathbf{A} and the sources \mathbf{s} . This is done by adaptively calculating the \mathbf{w} vectors and setting up a cost function which either maximizes the non-gaussianity of the calculated $s_k = \mathbf{w}^T \mathbf{x}$ or minimizes the mutual information. In certain circumstances, the cost function may employ a priori knowledge of the probability distributions of the sources [26].

The original sources \mathbf{s} can be recovered by multiplying the observed signals \mathbf{x} with the inverse of the mixing matrix $\mathbf{W} = \mathbf{A}^{-1}$, also known as the unmixing matrix. Here it is assumed that the mixing matrix is square ($n = m$). If the number of basis vectors is greater than the dimensionality of the observed vectors, $n > m$, the task is overcomplete but is still solvable with the pseudo inverse [26, 27].

Linear noisy ICA

With the added assumption of zero-mean and uncorrelated Gaussian noise $n \sim N(0, \text{diag}(\Sigma))$, the ICA model takes the form $\mathbf{x} = \mathbf{A}\mathbf{s} + n$.

Identifiability

The independent components are identifiable up to a permutation and scaling of the sources. This identifiability requires that [27]:

- At most one of the sources s_k is Gaussian,

- The number of observed mixtures, m , must be at least as large as the number of estimated components n : $m \geq n$. It is equivalent to say that the mixing matrix A must be of full rank for its inverse to exist.

Independent Component Analysis is one of the component-based methods which are extensively used in the pattern analysis and biosignal analysis. ICA separates the noises from the EEG signals by decomposing the signals into several independent components depending on statistical independence of signals. The advantage of ICA is that it does not require an additional channel reference since the algorithm itself does not require a priori information. However, ICA needs a visual inspection to identify the artifact independent components make it time consuming and subjective [28].

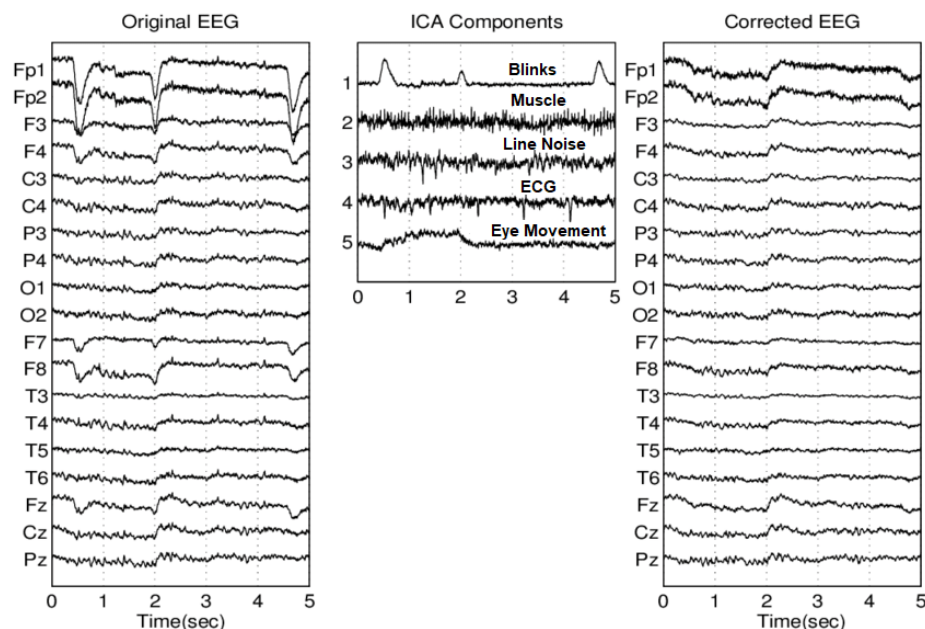


Figure 3.1 – Independent Component Analysis for EEG signal

After the elimination of the artifacts, the significant features of the EEG signals will be extracted using feature selection techniques. The feature extraction and selection techniques are important to identify certain properties that can effectively be used in classifying the EEG signals. There are several approaches used in feature extraction including time-domain analysis, frequency-domain analysis and time-frequency domain analysis. The features such as minimum, maximum, mean, standard deviation and energy are commonly used in time-domain analysis. The disadvantages of time-domain approach

are high sensitivity of the selected features and the demand for higher storage capabilities [24].

3.2 Fast Fourier Transform (FFT) Method

Spectral analysis of a signal involves decomposition of the signal into its frequency (sinusoidal) components. In other terms, spectral analysis techniques may be used to break the initial signal from its subspectral components. Since it is timeshift invariant, the Fourier transform is considered the best transition between time and frequency domains among spectral analysis techniques. The Fourier transform pairs are written as follows [29]:

$$X(k) = \sum_{n=0}^{N-1} x(n)W_N^{kn}$$

$$x(k) = \frac{1}{N} \sum_{n=0}^{N-1} X(n)W_N^{-kn}$$

where $W_N = e^{-j(2\pi/N)}$ and $N = \text{length}[x(n)]$.

The Fourier transforms of the EEG signals shown in Figure 3.2.

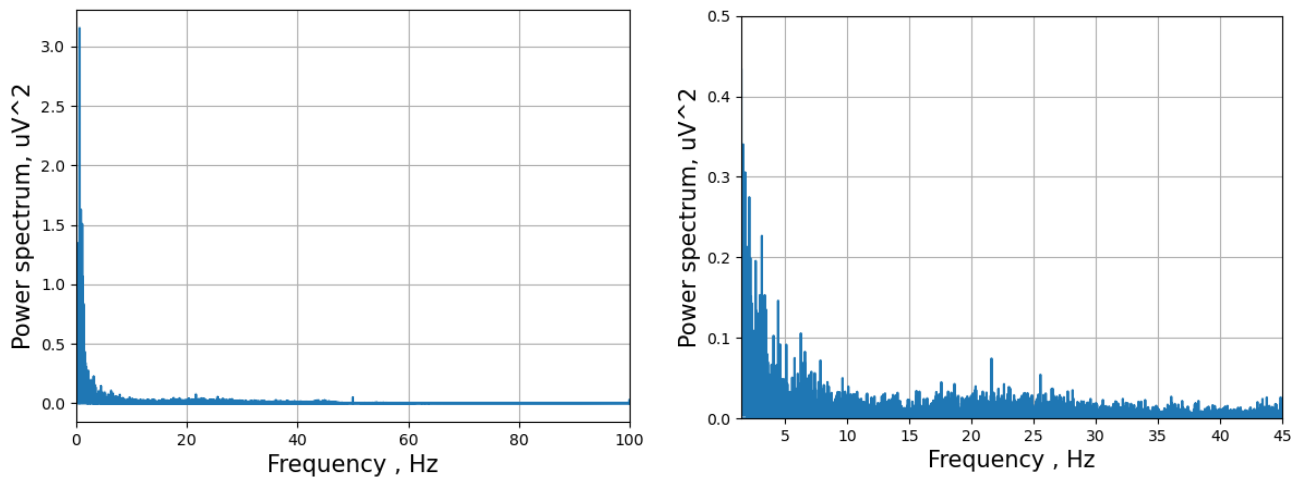


Figure 3.2 – Spectrum of the EEG signal: (a) Full scale; (b) “Main EEG bands” scale (1.5-45 Hz)

This method employs mathematical means or tools to EEG data analysis. Characteristics of the acquired EEG signal to be analyzed are computed by power spectral density (PSD) estimation in order to selectively represent the EEG samples signal [30].

3.3 Short-time Fourier Transform (STFT) Method

Spectrogram is the most often technique used to analyze signal in time-frequency domain. It is done by applying Short Time Fourier Transform (STFT) on a signal then mapping it into a two-dimensional function of frequency and time [31].

To compute the STFT, firstly, the signal is partitioned into several segments of short-time signals by shifting the time window with some overlapping. A Hamming window technique then applies to maintain the continuity between the beginning and the last points in the frames which can prevent leakage effect in the spectrum. Then Discrete Fourier Transform (DFT) is computed to each segment to acquire each local frequency spectrum. The general STFT equation is given by equation:

$$S(m, k) = \sum_{n=0}^{N-1} s(n + mN')w(n)e^{-j\frac{2\pi}{N}nk}$$

where $k = 0, 1, \dots, N - 1$

$S(m, k)$ indicates the m-index time-frequency spectrogram.

N – window segment length.

N' – the shifting step of the time window.

$w(n)$ – window method of an N -point sequence.

N' should be smaller than N in order to make overlap between time windows. This step is done to comprehensively capture the signal temporal features and changes. The spectrogram is defined as the magnitude of $S(m, k)$, which is represented as $A(m, k)$.

$$A(m, k) = \frac{1}{N} |S(m, k)|^2$$

STFT can give different results on spectrogram resolution issues. There exists contradiction in selection of time resolution and frequency resolution. Wide window length will give better frequency resolution but poor time resolution meanwhile narrower window length will give good time resolution but poor frequency resolution. By choosing appropriate window length and overlap, a better visualization in spectrogram can be obtained [32]. The spectrogram of the EEG signals is shown in Figure 3.3.

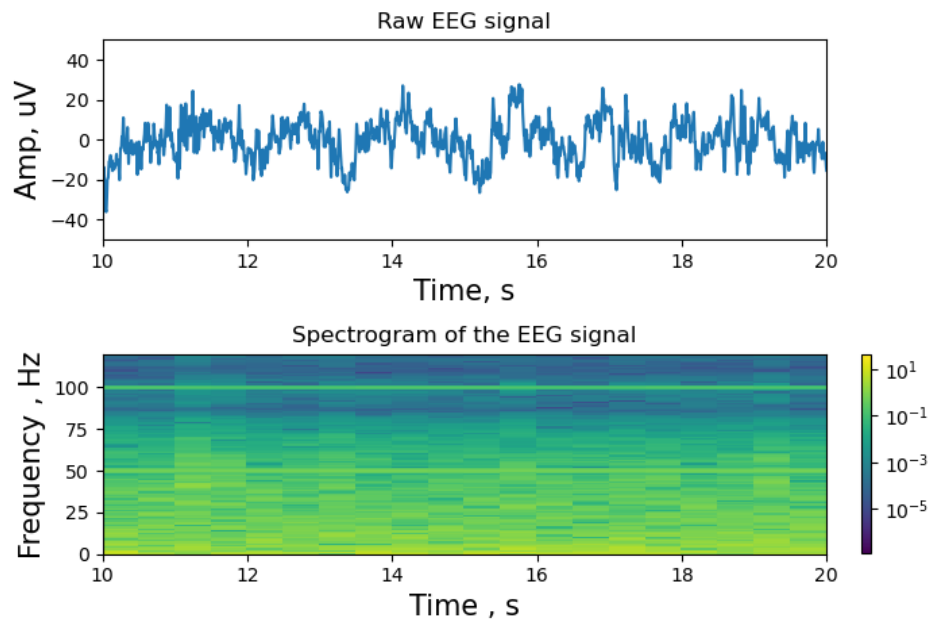


Figure 3.3 – Raw EEG signal and its spectrogram

3.4 Wavelet transform

Wavelet transform decomposes a signal into a set of functions called wavelets. These are obtained from a single prototype wavelet, called mother wavelet, by dilatations and contractions, as well as by shifts [33].

In a study written by Alfred Haar in 1909, the word "wavelet" was first used. Jean Morlet and his team at the Marseille Theoretical Physics Center, operating under Alex Grossmann in France, were the first to introduce the wavelet principle in its current theoretical form. Wavelet analysis techniques were mostly established by Y. Meyer and his collaborators, who also assured that the methods were widely distributed. Stephane Mallat's work in 1988 is the source of the key algorithm. Wavelet study has grown in popularity since then. Such study is especially involved in the United States, where scientists like Ingrid Daubechies, Ronald Coifman, and Victor Wickerhauser are leading the way.

On the basis of the input signal $x(t)$, WT may be continuous WT (CWT) or discrete WT (DWT). The CWT is expressed as $CWT(a, b) = \int x(t)\psi_{a,b}^*(t)dt$, where $*$ denotes the complex conjugate, a $a \in R$ represents the scale parameter, and $b \in R$ represents the translation. The function $\psi_{a,b}(t)$ is obtained by scaling the prototype wavelet $\psi(t)$ at time a and scale b , and is defined as $\psi_{a,b}(t) = \frac{1}{\sqrt{a}}\psi\left(\frac{t-b}{a}\right)$.

Generally, in wavelet applications, orthogonal dyadic functions are chosen as the mother wavelet. This transform is often discretized in a and b on a dyadic grid, with the time remaining continuous. The commonly used mother wavelet is defined as $\psi_{j,k}(t) = 2^{-j/2}\psi(2^{-j}t - k)$, where $\{\psi_{j,k}(t), j, k \in Z\}$ is for $L^2(R)$ [29].

Wavelet transforms of the EEG signals are shown in Figure 3.4. Also by using WT, one can view the shapes of the subspectral components of the EEG signal in time domain to be different from those in Fourier transform.

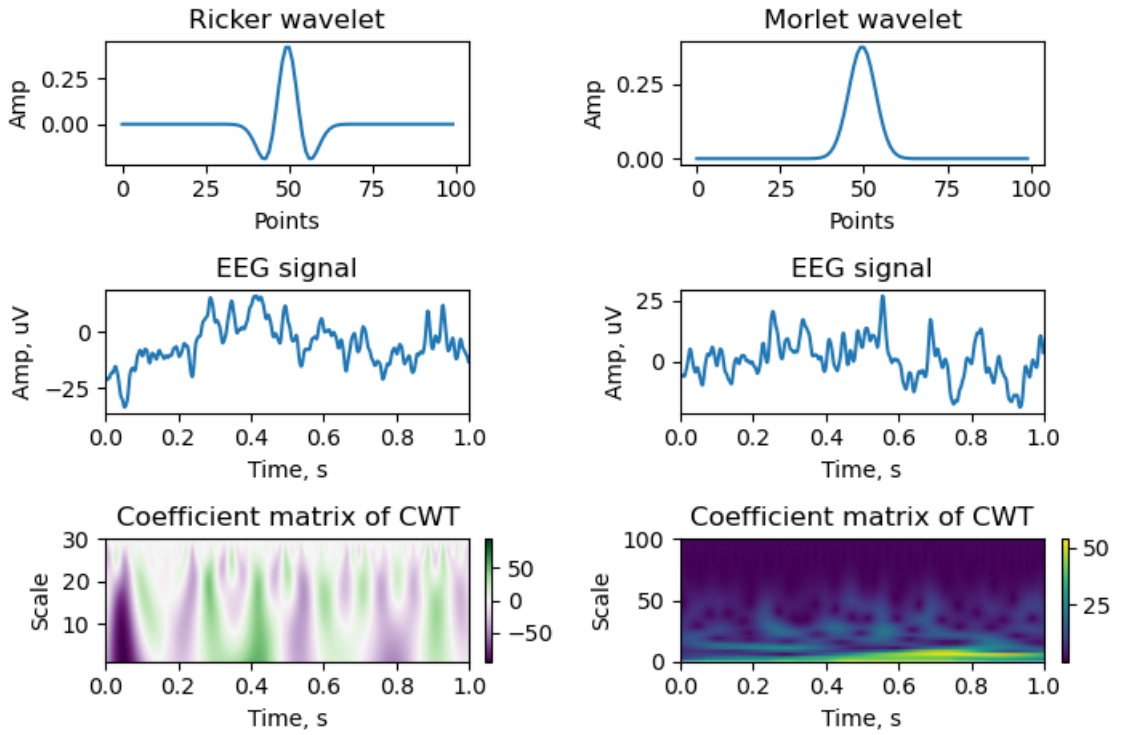


Figure 3.4 – Wavelet transform

3.5 Detrended fluctuation analysis (DFA)

The DFA method has become a used technique to determine the fractal scaling properties and the detection of long-range correlations in noisy and non-stationary time series. Detrended fluctuation analysis is a simple mathematical method but very efficient to investigate the power-law of long-term correlations of non-stationary time series. It is necessary to obtain the characteristics of the local fluctuations at different time-scales [34].

Detrended Fluctuation Analysis is a technique for measuring the same power law scaling observed through R/S Analysis. It was introduced specifically to address non-stationaries. Like R/S Analysis, a synthetic walk is created, however a detrending operation is performed where a polynomial (originally and usually, linear) is locally fit to the walk within each window to identify the trend and then that trend is subsequently removed. DFA is typically described as enabling correct estimation of the power law scaling (Hurst exponent) of a systems' signal in the presence of (extrinsic) non-stationaries while eliminating spurious detection of long-range dependence. This purported protection against non-stationaries effects is attributed to the “detrending” operation performed and is thought to provide an important distinction from spectral or other approaches. Empirically, it has been found that when estimating scaling in well-defined test cases, such as fractional Brownian noise, DFA performs well compared to other heuristic techniques, including R/S Analysis and is competitive, in the limit of large window sizes. The combination of DFA being specifically designed to seamlessly deal with non-stationaries (intent) and its relatively good performance on simple test cases (observation) has solidified the opinion that DFA is effectively a turn-key approach: one can simply feed data in and obtain a meaningful parameterization as embodied by the scaling parameter (Hurst exponent). As a result, DFA is a popular approach and is specifically chosen if non-stationaries are either suspected or known to exist [35].

DFA algorithm consists of two steps:

- 1) the data series $x(k)$ is shifted by the mean and integrated (cumulatively summed), $y(k) = \sum_{i=1}^k (x(i) - \langle x \rangle)$, then segmented into windows of various sizes Δn ;
- 2) in each segmentation the integrated data is locally fit to a polynomial $y_{\Delta n}(k)$ (originally and typically, linear) and the mean-squared residual $F(n)$ (“fluctuations”) is found: $F(n) = \sqrt{\frac{1}{N} \sum_{k=1}^N [y(k) - y_n(k)]^2}$, where N is the total number of data points. Note that $F^2(n)$ can be viewed as the average of the summed squares of the residual found in the windows. The n -th order polynomial regressor in the DFA family is typically denoted as DFA n , with unlabeled DFA often referring to DFA.

This procedure tests for self-similarity (fractal properties) as it performs a measure (the dispersion of the residual of integrated fluctuations about a regressor) at different resolutions (window sizes). If power law scaling is present then a double logarithmic (“log-log”) plot of $F(n)$ versus n , often termed the fluctuation plot, is expected to be linear and a scaling exponent α can be estimated from a least-squares fit. This scaling exponent α is a measure of correlation in the noise and is simply an estimate of the Hurst exponent H .

The standard view, following the original reasoning, is that by removing local polynomials non-stationaries can be “detrended” [35].

The scaling exponent α is calculated as the slope of a straight line fit to the log-log graph of n against $F(n)$ using least-squares. The Hurst exponent has been generalized into this exponent. Because the expected displacement in an uncorrelated random walk of length N grows like \sqrt{N} , an exponent of $\frac{1}{2}$ would correspond to uncorrelated white

noise. The outcome is fractional Gaussian noise when the exponent is between 0 and 1, with the exact value providing information about the series self-correlations [36]:

- $\alpha < 1/2$: anti-correlated
- $\alpha \approx 1/2$: uncorrelated, white noise
- $\alpha > 1/2$: correlated
- $\alpha \approx 1$: 1/f-noise, pink noise
- $\alpha > 1$: non-stationary, unbounded
- $\alpha \approx 3/2$: Brownian noise

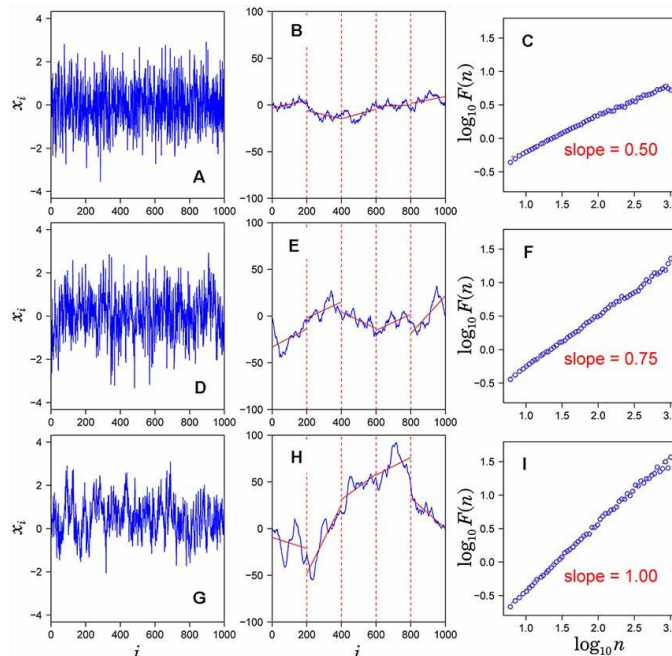


Figure 3.5 – Assessment of scaling exponents of time series x_i by detrended fluctuation analysis (DFA). (A,D,G) Examples of time series. (B,E,H) Integrated series (blue solid lines) of the time series shown in the left hand panel. (C,F,I) Log-log plot of $F(n)$ vs. n . The scaling exponent α is estimated by the slope of the linear fit (red dashed lines) [37]

3.5.1 Detrending moving average (DMA) algorithm

According to the DFA, the time series is first divided in boxes of equal lengths, then trends are estimated as least-squares polynomial fitting of different orders m in each non-overlapping and equally spaced box of length n . The DMA algorithm has been proposed as an alternative technique to quantify long-range correlations.

The main ingredient of the DMA algorithm is the generalized variance $\sigma_{DMA}^2(n)$ of the time series $\{y(i)\}_{i=1}^N$ with respect to the trend $\{\tilde{y}_n(i)\}$ at scale n :

$$\sigma_{DMA}^2(n) = \frac{1}{N-n+1} \sum_i [y(i) - \tilde{y}_n(i)]^2, \quad (3.1)$$

where $\tilde{y}_n(i)$ is defined as a time-dependent average function of $y(i)$. In the simplest case, called backward DMA, $\tilde{y}_n(i)$ can be estimated as the ordinary moving average: $\tilde{y}_n(i) = \frac{1}{n} \sum_{k=0}^{n-1} y(i-k)$, and the range of the summation in (3.1) is from n to N [38].

For random walk-type processes with diffusive behavior, such as the fractional Brownian motion, the power-law increase of the root-mean square deviation $\sigma_{DMA}(n)$ with the moving average window size n : $\sigma_{DMA}(n) \sim n^\alpha$, provides an estimate of the scaling exponent α and thus of the Hurst exponent H . For long-range correlated time series $\{x(i)\}_{i=1}^N$ with non-diffusive behavior, such as fractional Gaussian noise, the integrated series (cumulative sum), $y(i) = \sum_{j=1}^i x(j)$, as a sample path of a random walk driven by $\{x(i)\}$ is investigated and quantified in terms of the scaling exponent α .

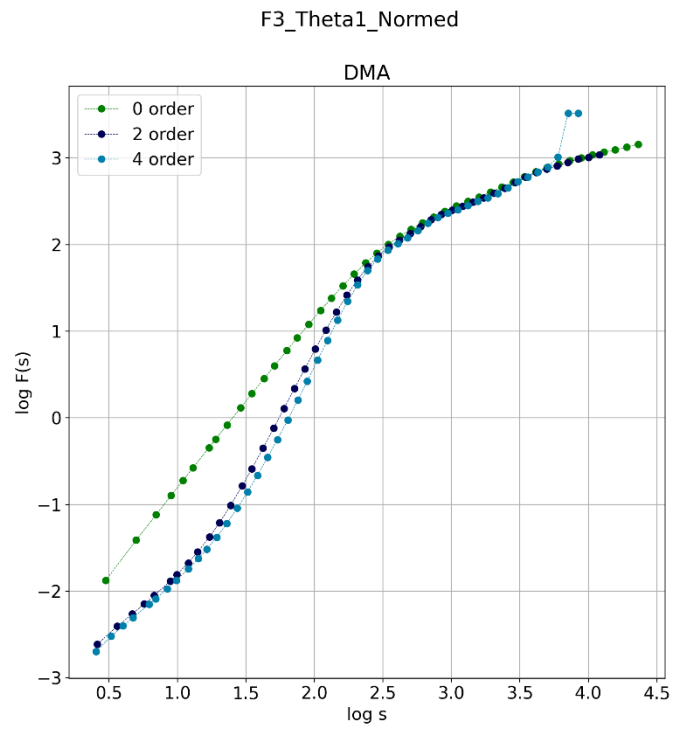


Figure 3.6 – Graph of DMA analysis of EEG signal in “log-log” scale

3.6 Conclusions for Chapter 3

In this chapter main math methods of EEG analysis were shown in combination with practical examples that were visualized using Python programming language. Every method helps to extract special patterns from the raw EEG signal: it can be spectral powers, artefacts or pathological elements in frequency bands, some similarities during all records, etc.

For instance, spectral analysis (done by the Fast Fourier Transform (FFT)) of the signal involves the decomposition of the signal into its frequency (sinusoidal) components. In other words, the output signal can be divided into its subspectral components using spectral analysis methods. Then, spectrogram is the most popular type of analysis used to study the signal in the frequency-time domain. This is done by applying a Short-Time Fourier Transform (STFT) to the signal and then mapping it to a two-dimensional frequency and time function. Wavelet analysis is useful in detecting special patterns (called wavelets) in the EEG signals. DMA/DFA is a simple mathematical method, but very effective for studying the law of long-term correlations of nonstationary time series.

4 ANALYSIS OF BRAIN REACTION TO EMOTIONAL FACES

Facial expressions are considered to be one of the most complex and evolutionary-important visual stimuli, endowed with a wide range of characteristics and attributes for the brain to process. According to recent discoveries, our ability to detect, recognize and evaluate facial expression is an integrative product of experience and inherited predisposition, which both shape perception [39].

Our current study aimed to discover the short-term alterations in the neural mechanisms mediating the perception of emotionally neutral faces, caused by the emotional background of either positive or negative valence. To do that, EEG-data was collected during the presentation of the relevant visual stimuli and was further analyzed with Power Spectrum Density (PSD) to discover the strength of activation and Detrending Moving Average (DMA) method to discover long-range spatiotemporal correlations in EEG.

4.1 Subjects and data collection

48 healthy volunteer students of Taras Shevchenko National University of Kyiv (29 females) aged 18-24 (Mean age = 21, SD=1,76) participated in the study. The participants were enrolled in the study based on the following exclusion criteria: addiction to psychoactive substances, clinical manifestations of mental, cognitive, or neurological impairments, use of psychiatric medications, visual system lesions (impaired acuity, color blindness).

The image demonstration procedure and recording of the cerebral cortex's induced activity were performed using the software and hardware complex "Neurocom" (KhAI Medica, Kharkiv, Ukraine) according to a specially created template. Electrodes were applied to the scalp following the international "10-20" system.

4.2 Experiment design

The EEG data was recorded during the sequential demonstration of four 3-minute-long image series, where a single stimulus was on-screen for 5 sec. The experimental design was organized so that each series containing (1) neutral stimuli was preceded by (2) positive and (3) negative images. Examples of images shown on Figure 4.1. Recordings were also made during the resting state with both closed and open eyes.



Figure 4.1 – Examples of images for stimulating: (1) – neutral, (2) – positive, (3) – negative

Stimuli were selected from the International Affective Pictures System (IAPS) based on their average emotional valence values. Therefore, neutral emotional faces ($M = 4.22$, $SD = 1.64$ to $M = 5.84$, $SD = 1.62$) were demonstrated among positive ($M = 6.94$, $SD = 1.42$ to $M = 8.03$, $SD = 1.13$) and negative ($M = 4.22$, $SD = 1.64$ to $M = 5.84$, $SD = 1.62$) emotional faces.

In order to assess the induced changes of the brain's electrical activity, the EEG-bands were subdivided in a following way: θ_1 [3.5, 5.8], θ_2 [5.9, 7.4], α_1 [7.5, 9.4], α_2 [9.5, 10.7], α_3 [10.8, 13.5], β_1 [13.6, 25], β_2 [25.1, 40] Hz. The following analysis methods were applied to each EEG band separately.

4.3 Methods used for analysis of brain activity

4.3.1 Power spectral density estimation

EEG signals for all types of visual stimuli were analyzed using the power spectral density (PSD).

First, Fast Fourier Transform was used to obtain the spectrum, which was squared to obtain the estimate of PSD. The average powers of EEG were calculated for all channels in the abovementioned frequency bands. Normalized powers for each band were obtained by summarizing powers in particular frequency ranges according to selected for the study. These sums of powers were divided by the total power of the whole signal, so, finally, normalized powers were obtained.

4.3.2 Detrended moving average analysis

The Detrending Moving Average (DMA) algorithm has been widely used in its several variants for characterizing long-range correlations of random signals and sets (one-dimensional sequences or high-dimensional arrays) either in time or spatial domains.

To get the DMA of EEG components in particular frequency range, first the 4th order Butterworth bandpass filter was used, with the passband matched to the required frequency range. Then, for each filtered signal the analytic signal was obtained by the Hilbert Transform, to get the envelope as an absolute value of the analytic signal [40]. Further, the envelope was used to perform the DMA analysis.

By the DMA analysis long-range correlation properties of EEG signals over time were found. Scaling exponents, estimated from DMA analysis log-log plots, were calculated and were shown on the head's map for all necessary channels and frequency bands.

4.3.3 Statistical significance evaluation

Statistically significant differences in PSD and scaling exponents distributions were obtained for trials during perception of neutral faces preceded by positive (n1) and negative (n2) images.

For PSD values in every frequency range, the Wilcoxon signed-rank test (testing two generalized n1/n2 trials without gender separation) and Mann-Whitney rank test (testing female/male groups for the same set of trails) were used to identify the channels for which the median values of the attributes were significantly different for both trials (n1, n2). The difference between medians was then determined for these channels, and its map throughout the skull surface was examined. The visualization was the following: if the difference between medians was greater than 0, “+1” was assigned for the corresponding EEG channel, if the difference was less than 0, “-1” was assigned, if there were not any significant differences “0” was assigned. As a result, the map across the head surface was obtained.

The statistical tests for DMA scaling exponents were conducted in the same way. If the median value of the scaling exponent for n1 trial is statistically different from that in n2 trial in some channel, it is used for further analysis.

As all frequency bands (θ_1 , θ_2 , α_1 , α_2 , α_3 , β_1 , β_2) that were analyzed in this work are derived from the same EEG recording, p-value correction was applied. To account for the multiple comparisons using step down method using Sidak adjustments [41] was used.

4.4 Experiment results

For visualization purposes, the head heatmaps were used. First, the values were normalized between minimal and maximum values, so differences in color showed main features of signals clearly.

As a result, PSDs were visualized as a map on the schematic figure of the head used to make the statistical significance evaluation that showed that differences in powers for our signals were not accidental but caused by non-identical types of visual impact. These data were shown in the heads maps as well.

The analysis of power spectrum density alterations revealed neurodynamics elicited by visual stimuli perception (Figure 4.2). However, the comparison of PSD values obtained during the demonstration of the first and second neutral series showed the formation of a well-pronounced activation focus in the left parietal region of the cortex (P3) in $\theta 2$ subband while processing neutral images preceded by negative stimuli (Figure 4.3). This evidence allows us to assume that the negative emotional context enhances verbalization and association-related cognitive processes, while positive background increases memory-related neurodynamics.

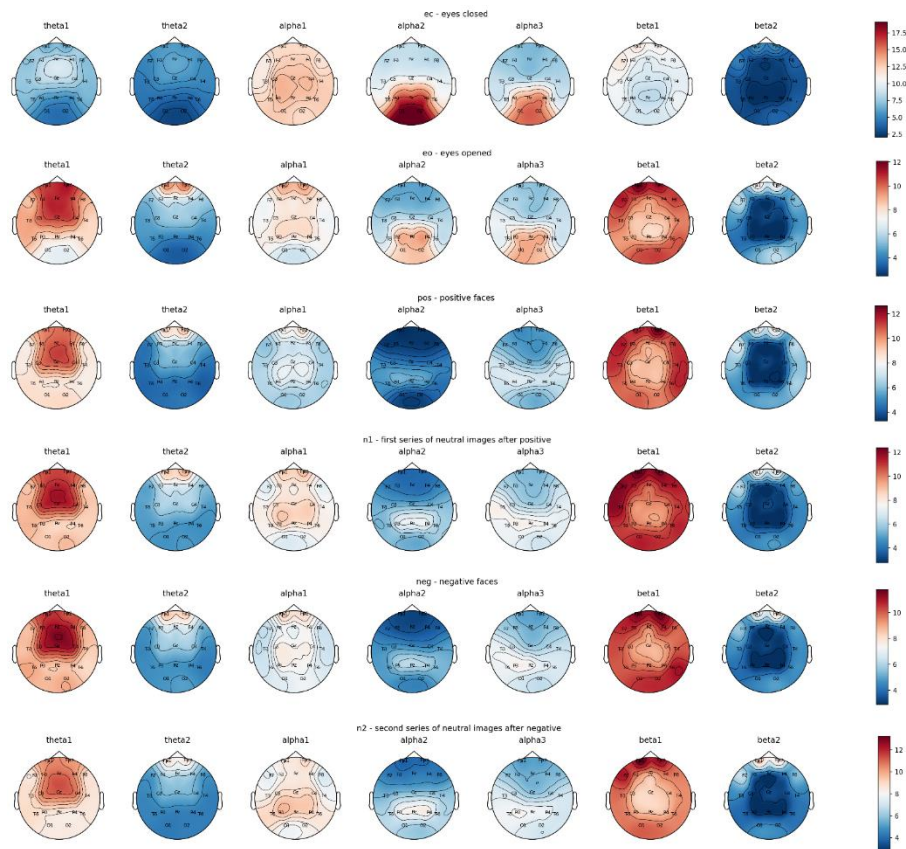


Figure 4.2 – Topographic distribution of PSD values during perception of different stimulus

The comparison made between the male and female (Figure 4.3) experimental groups demonstrated that in men both positive and negative emotional backgrounds significantly increased activation processes within the prefrontal and frontal cortical regions in the β_2 subband, which marked the increase in internal attention, verbalization, and emotional regulation mechanisms [42]. At the same time, in the β_1 subband, a pronounced generalization of enhanced activation among the majority of cortical regions in the male group reflected the increase in visual spatial attention-related processes.

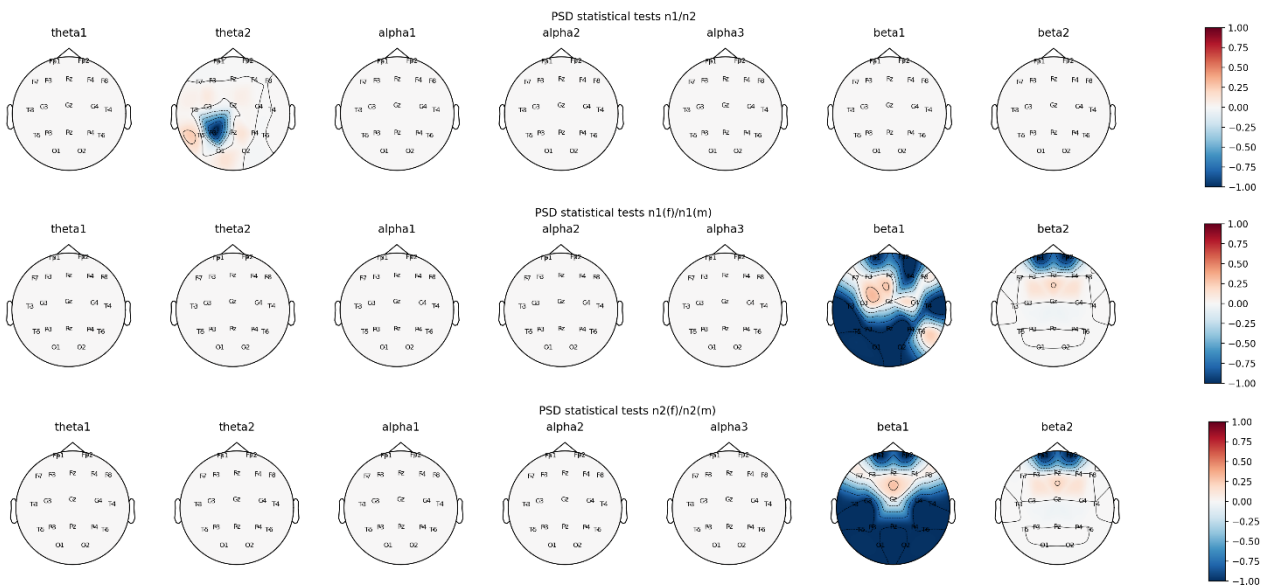


Figure 4.3 – Regions of statistically significant differences of PSD values

Results obtained using the DMA algorithm showed statistically significant differences in left temporal and frontal areas of the cortex, which were characterized by a more pronounced activation during the perception of neutral faces in the context formed by positive images (Figure 4.4 and Figure 4.5). This might mark the enhancement of inner attention and positive emotional experience trail [43].

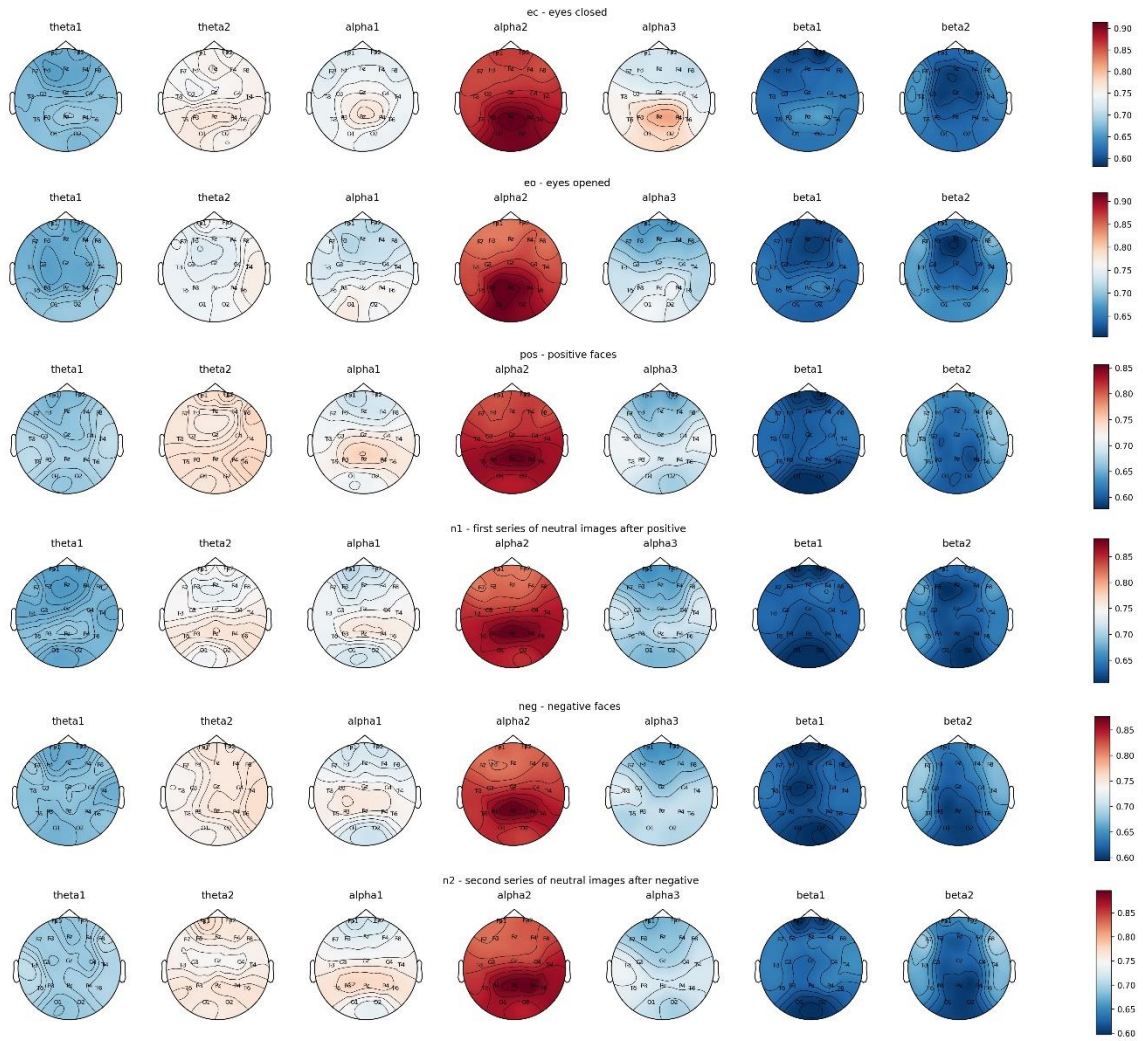


Figure 4.4 – Topographic distribution of DMA alpha values during perception of different stimulus

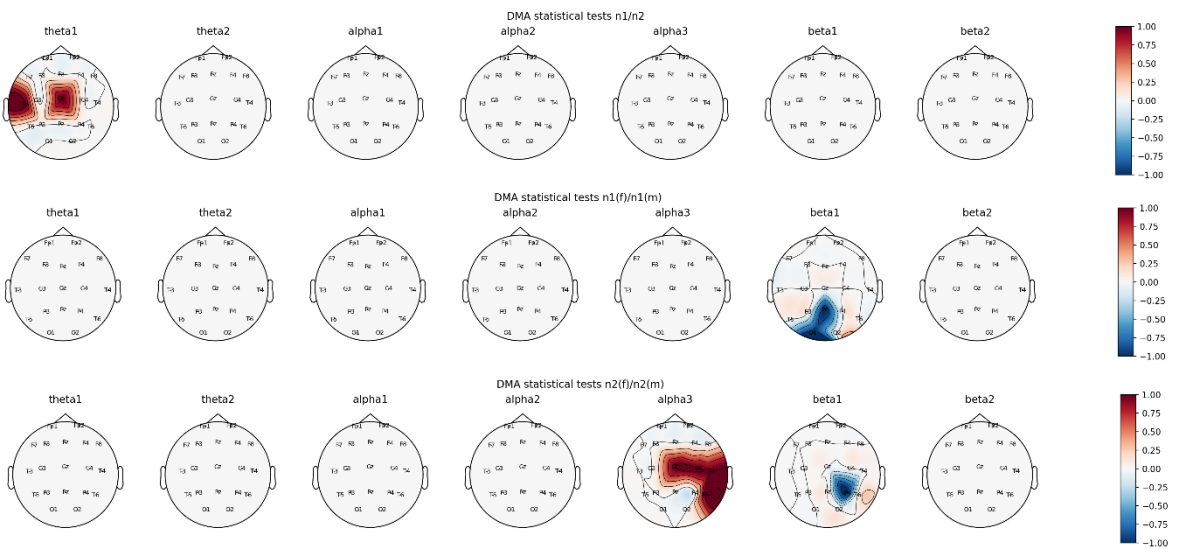


Figure 4.5 – Regions of statistically significant differences of DMA alpha values

Intergroup analysis demonstrated that the male group had significantly increased activation levels in occipito-parietal cortical regions within the $\beta 1$ EEG-subband when processing the neutral faces in the presence of positive background, which once again highlights the increased activity of the cognitive beta-network. A similar picture in the $\beta 1$ subband was observed during the analysis of the neutral image processing modulated by negative emotional context. However, in women, a wide network of connections covering temporal, central, and frontal regions was detected in the $\alpha 3$ subband, which might be explained by specific working memory mechanisms and lack of downstream cortical control and suppressive function of attention upon mental imagery and emotions [44].

4.5 Conclusions for Chapter 4

In this chapter real experimental EEG data were analyzed by using special methods such as Power spectral density (PSD) estimation, Detrended Moving Average (DMA) analysis and Statistical significance evaluation.

As a result, the analysis of the EEG-based brain neurodynamics in the process of perception of human faces of different modalities revealed the sex-related manifestations of the emotional valence influence on neutral face perception. The main differences consisted in the activation of two major cognitive networks of the brain: emotional or theta-network and cognitive beta-network. Thus, whereas the data obtained from PSD values distribution is suitable for evaluating alterations in cortical activation and inhibition processes, the DMA method is able to provide information about the cortical networks' functioning stability.

CONCLUSIONS

The study of electrical potentials in the brain holds a significant role in the understanding of brain function. Electroencephalography is a branch of electrophysiology that studies the patterns of the total electrical activity of the brain removed from the surface of the skin of the scalp, as well as the method of recording such potentials. Also, EEG is a non-invasive method for studying the functional state of the brain by registering its bioelectric activity.

Electroencephalography measures voltage fluctuations resulting from ion current in neurons in the brain. Clinically, an electroencephalogram is a graphic representation of the spontaneous electrical activity of the brain over a period of time, recorded from multiple electrodes on the brain or the surface of the scalp. EEG is a sensitive method of investigation, it reflects the slightest changes in the function of the cerebral cortex and deep brain structures in the time dimension, providing millisecond time resolution that is not available to other methods of studying brain activity.

Electroencephalography provides a qualitative and quantitative analysis of the functional state of the brain and its reactions to the action of stimuli. EEG recording is widely used in diagnostic and therapeutic work (especially often in epilepsy), in anesthesiology, as well as in the study of brain activity associated with the implementation of functions such as perception, memory, adaptation, etc.

On the electroencephalograms, the rhythmicity of the electrical activity of the brain is noticeable. There are a number of rhythms, denoted by the letters of the Greek alphabet. Electroencephalography is also used to identify event — related potentials-brain responses that are the direct result of a particular sensation, cognitive, or motor event.

The electrical function in the human brain is the subject of the work. Methods of studying electroencephalograms during the operation of different stimuli are the focus of the project. The aim is to learn more about the origin of brain electrical impulses, as well as the methods for registering and analyzing them, in order to better understand how the brain responds to visual emotional stimuli.

Initially the EEG records were made for 48 healthy volunteers whose EEG recording was performed during seeing emotionally charged visual stimulation. The International Affective Pictures System (IAPS) was used to select stimuli depending on their average emotional valence values. The EEG-bands is subdivided in the following way to measure the mediated differences in brain electrical activity: $\theta 1$ [3.5, 5.8], $\theta 2$ [5.9, 7.4], $\alpha 1$ [7.5, 9.4], $\alpha 2$ [9.5, 10.7], $\alpha 3$ [10.8, 13.5], $\beta 1$ [13.6, 25], $\beta 2$ [25.1, 40] Hz.

As a consequence, PSDs is visualized as a map on the graphical figure of the head used to make the statistical significance examination, showing that differences in signal powers were induced by non-identical modes of visual influence rather than being an accident. The heads charts also included this info.

The analysis of differences in power spectrum density revealed that visual stimuli activated neurodynamics. When comparing PSD values obtained during the first and second neutral sequence presentations, it was discovered that when processing neutral images accompanied by negative stimulation, a well-defined arousal focus emerged in the left parietal area of the cortex in the $\theta 2$ subband. This research suggests that a negative emotional context improves verbalization and association-related cognitive functions, while a favorable emotional context improves memory-related neurodynamics.

Both positive and negative emotional backgrounds substantially enhanced activation processes within the prefrontal and frontal cortical regions in the $\beta 2$ subband in males, indicating an improvement in internal focus, verbalization, and emotional control mechanisms. Simultaneously, in the $\beta 1$ subband, the male community showed a marked generalization of increased activity across the plurality of cortical areas, indicating an improvement in perceptual spatial attention-related processes.

In the presence of positive images, the DMA algorithm showed statistically significant differences in the left temporal and frontal regions of the cortex, which were characterized by more pronounced activation during the detection of neutral faces. This may be the beginning of a new journey toward greater inner concentration and positive interpersonal interactions.

When processing neutral faces in the midst of a positive context, intergroup research revealed that the male group had slightly higher activation levels in occipito-

parietal cortical regions within the β_1 EEG-subband, highlighting the enhanced involvement of the cognitive beta-network once again. During the study of neutral image processing modulated by negative emotional meaning, a related picture was found in the β_1 subband. However, in the α_3 subband, a large network of associations spanning temporal, middle, and frontal regions was observed in women, which may be clarified by complex working memory processes and a loss of downstream prefrontal regulation and suppressive role of concentration on mental imagery and emotions.

The sex-related manifestations of the emotional valence effect on neutral face perception were discovered by analyzing EEG-based brain neurodynamics in the process of perception of human faces of various modalities. The stimulation of two large cognitive networks in the brain: mental or theta-network and cognitive beta-network, was the key distinction. Thus, although the PSD value distribution evidence is useful for assessing changes in cortical stimulation and inhibition mechanisms, the DMA approach may provide knowledge about the cortical networks' working stability.

REFERENCES

1. C. Chiron, I. Jambaque, R. Nabbout, R. Lounes, A. Syrota, O. Dulac The right brain hemisphere is dominant in human infants. *Brain* 1997. <https://doi.org/10.1093/brain/120.6.1057>
2. Niedermeyer E.; da Silva F.L. (2004). *Electroencephalography: Basic Principles, Clinical Applications, and Related Fields*. Lippincott Williams & Wilkins. ISBN 978-0-7817-5126-1
3. J. Satheesh Kumar P. Bhuvaneshwari Analysis of Electroencephalography (EEG) Signals and Its Categorization—A Study <https://doi.org/10.1016/j.proeng.2012.06.298>
4. Obermaier, B., Neuper, C., Guger, C., & Pfurtscheller, G. (2001). Information transfer rate in a five-classes brain-computer interface. *IEEE Transactions on Neural Systems and Rehabilitation Engineering*, 9(3), 283–288. <https://doi:10.1109/7333.948456>
5. Birbaumer, N. (2006). Brain–computer-interface research: Coming of age. *Clinical Neurophysiology*, 117(3), 479–483. doi:10.1016/j.clinph.2005.11.002
6. Kim, S.-P., Rao, Y. N., Erdogmus, D., Sanchez, J. C., Nicolelis, M. A. L., & Principe, J. C. (2005). Determining Patterns in Neural Activity for Reaching Movements Using Nonnegative Matrix Factorization. *EURASIP Journal on Advances in Signal Processing*, 2005(19). doi:10.1155/asp.2005.3113
7. Sanei, S. and Chambers, J. A. 2007. *EEG Signal Processing*. John Wiley & Sons, Incorporated
8. Nowlis, D. P., & Kamiya, J. (1970). THE CONTROL OF ELECTROENCEPHALOGRAPHIC ALPHA RHYTHMS THROUGH AUDITORY FEEDBACK AND THE ASSOCIATED MENTAL ACTIVITY. *Psychophysiology*, 6(4), 476–484. doi:10.1111/j.1469-8986.1970.tb01756.x
9. Taheri, B. A., Knight, R. T., & Smith, R. L. (1994). A dry electrode for EEG recording. *Electroencephalography and Clinical Neurophysiology*, 90(5), 376–383. doi:10.1016/0013-4694(94)90053-1

10. Ng S.C., Raveendran P. (2007) Comparison of different Montages on to EEG classification. In: Ibrahim F., Osman N.A.A., Usman J., Kadri N.A. (eds) 3rd Kuala Lumpur International Conference on Biomedical Engineering 2006. IFMBE Proceedings, vol 15. Springer, Berlin, Heidelberg. https://doi.org/10.1007/978-3-540-68017-8_93
11. Pinho, F.; Correia, J.H.; Sousa, N.J.; Cerqueira, J.J.; Dias, N.S. Wireless and wearable EEG acquisition platform for ambulatory monitoring. In Proceedings of the IEEE 3rd International Conference on Serious Games and Applications for Health (SeGAH), Rio de Janeiro, Brazil, 14–16 May 2014.
12. Feng, S.; Tang, M.; Quivira, F.; Dyson, T.; Cuckov, F.; Schirner, G. EEGu2: An embedded device for brain/body signal acquisition and processing. In Proceedings of the International Symposium on Rapid System Prototyping (RSP), Pittsburgh, PA, USA, 1–7 October 2016.
13. Senevirathna, B.; Berman, L.; Bertoni, N.; Pareschi, F.; Mangia, M.; Rovatti, R.; Setti, G.; Simon, J.; Abshire, P. Low cost mobile EEG for characterization of cortical auditory responses. In Proceedings of the 2016 IEEE International Symposium on Circuits and Systems (ISCAS), Montreal, QC, Canada, 22–25 May 2016.
14. Vo, T.T.; Nguyen, N.P.; Vo Van, T. WEEGEE: Wireless 8-Channel EEG Recording Device. In Proceedings of the BME 2017: 6th International Conference on the Development of Biomedical Engineering in Vietnam (BME6), Ho Chi Minh, Vietnam, 27–29 June 2017; Volume 63.
15. Wild, M.; Pegan, R. Wearable Bluetooth Brain-Computer Interface for Detection and Analysis of Ear-EEG Signals. 2015. Available online: <https://www.semanticscholar.org/paper/Wearable-BluetoothBrain-Computer-Interface-for-and-Wild-Pegan/bae82d84b4384bd86cf942139ac9a45326f3083d>
16. <https://www.olimex.com/Products/Breadboarding/BB-PWR-3608/resources/MT3608.pdf>
17. <https://mysku.ru/blog/aliexpress/37152.html>
18. https://www.ti.com/lit/ug/slau443b/slau443b.pdf?ts=1608199602672&ref_url=https%253A%252F%252Fwww.google.com%252F

19. https://www.ti.com/lit/ds/symlink/tps7a20.pdf?ts=1608198267678&ref_url=https%253A%252F%252Fru.mouser.com%252F
20. https://www.ti.com/lit/ds/symlink/ads1299.pdf?ts=1608125125093&ref_url=https%253A%252F%252Fwww.ti.com%252Fproduct%252FADS1299%253Futm_source%253Dgoogle%2526utm_medium%253Dcpc%2526utm_campaign%253Dasc-null-null-GPN_EN-cpc-pf-google-eu%2526utm_content%253DADS1299%2526ds_k%253DADS1299%2BDatasheet%2526DCM%253Dyes%2526gclid%253DCjwKCAiA_eb-BRB2EiwAGBnXXhqkxrGid-jhg9crlUQxg0AA5S4x4YJ83HaQ6qcjC3puLqL6cnJ6pxoC23kQAvD_BwE%2526gclidsrc%253Daw.ds
21. <https://www.silabs.com/documents/public/data-sheets/CP2102-9.pdf>
22. <https://arduinoinfo.mywikis.net/wiki/MegaQuickRef>
23. https://components101.com/sites/default/files/component_datasheet/ESP12E%20Datashheet.pdf
24. Abd Rahman, F., Othman, M. F., & Shaharuddin, N. A. (2015). Analysis Methods of EEG Signals: A Review in EEG Application for Brain Disorder. *Jurnal Teknologi*, 72(2). doi:10.11113/jt.v72.3886
25. Hyvarinen, A. (2012). Independent component analysis: recent advances. *Philosophical Transactions of the Royal Society A: Mathematical, Physical and Engineering Sciences*, 371(1984), 20110534–20110534. doi:10.1098/rsta.2011.0534
26. Lisha Sun, Ying Liu, & Beadle, P. J. (n.d.). Independent component analysis of EEG signals. *Proceedings of 2005 IEEE International Workshop on VLSI Design and Video Technology*, 2005. doi:10.1109/iwvdt.2005.1504590
27. https://en.wikipedia.org/wiki/Independent_component_analysis
28. Hyvarinen, A. (1999). Fast and robust fixed-point algorithms for independent component analysis. *IEEE Transactions on Neural Networks*, 10(3), 626–634. doi:10.1109/72.761722
29. Akin, M. (2002). *Journal of Medical Systems*, 26(3), 241–247. doi:10.1023/a:1015075101937

30. Al-Fahoum, A. S., & Al-Fraihat, A. A. (2014). Methods of EEG Signal Features Extraction Using Linear Analysis in Frequency and Time-Frequency Domains. *ISRN Neuroscience*, 2014, 1–7. doi:10.1155/2014/730218
31. Oppenheim, "Discrete-Time Signal Processing," Pearson Education, pp. 714-715.
32. Zabidi, A., Mansor, W., Lee, Y. K., & Che Wan Fadzal, C. W. N. F. (2012). Short-time Fourier Transform analysis of EEG signal generated during imagined writing. 2012 International Conference on System Engineering and Technology (ICSET). doi:10.1109/icsengt.2012.6339284
33. Hazarika, N., Chen, J. Z., Ah Chung Tsoi, & Sergejew, A. (n.d.). Classification of EEG signals using the wavelet transform. *Proceedings of 13th International Conference on Digital Signal Processing*. doi:10.1109/icdsp.1997.627975
34. Márton, L. F., Brassai, S. T., Bakó, L., & Losonczy, L. (2014). Detrended Fluctuation Analysis of EEG Signals. *Procedia Technology*, 12, 125–132. doi:10.1016/j.protcy.2013.12.465
35. Bryce, R. M., & Sprague, K. B. (2012). Revisiting detrended fluctuation analysis. *Scientific Reports*, 2(1). doi:10.1038/srep00315
36. https://en.wikipedia.org/wiki/Detrended_fluctuation_analysis
37. Seleznov, I., Zyma, I., Kiyono, K., Tukaev, S., Popov, A., Chernykh, M., & Shpenkov, O. (2019). Detrended Fluctuation, Coherence, and Spectral Power Analysis of Activation Rearrangement in EEG Dynamics During Cognitive Workload. *Frontiers in Human Neuroscience*, 13. doi:10.3389/fnhum.2019.00270
38. Carbone, Anna & Kiyono, Ken. (2016). Detrending Moving Average Algorithm: Frequency Response and Scaling Performances. *Physical Review E*. 93. 10.1103/PhysRevE.93.063309.
39. Isabel Gauthier, Rankin W. McGugin, Jennifer J. Richler, Grit Herzmann, Magen Speegle, Ana E. Van Gulick; Experience moderates overlap between object and face recognition, suggesting a common ability. *Journal of Vision* 2014;14(8):7. doi: <https://doi.org/10.1167/14.8.7>

40. Feldman, M. (2008). Hilbert Transform, Envelope, Instantaneous Phase, and Frequency. Encyclopedia of Structural Health Monitoring. doi:10.1002/9780470061626.shm046
41. Šidák, Z. K. (1967). "Rectangular Confidence Regions for the Means of Multivariate Normal Distributions". Journal of the American Statistical Association. 62 (318): 626–633. doi:10.1080/01621459.1967.10482935
42. Soleymani, M., Pantic, M., and Pun, T. (2012). Multimodal emotion recognition in response to videos. IEEE transactions on affective computing, 3(2), pp. 211-2239
43. Klimesch W. (1999). EEG alpha and theta oscillations reflect cognitive and memory performance: a review and analysis. Brain Res. Rev. 29, 169–195. 10.1016/s0165-0173(98)00056-3
44. Klimesch W. (1999). EEG alpha and theta oscillations reflect cognitive and memory performance: a review and analysis. Brain Res. Rev. 29, 169–195. 10.1016/s0165-0173(98)00056-3